CERN-TH.5902/90

QCD and Jets at LEP†

Torbjörn Sjöstrand
CERN — Geneva

Abstract:
The various aspects of our understanding of QCD in the context of LEP are discussed. Perturbative QCD may be described either in a matrix element approach or in a parton shower one, each with its advantages and drawbacks. The nonperturbative hadronization is not understood from first principles, but is modelled with string, cluster or independent fragmentation. Existing data from PETRA, PEP, TRISTAN and, most recently, LEP has been used to test and constrain the models that have been developed. The plan of these lecture is as follows:

- 1. Introduction
- 2. Perturbative QCD
  - 2.1. Matrix Elements
  - 2.2. Parton Showers
  - 2.3. Testing QCD
- 3. Fragmentation Models
  - 3.1. String Fragmentation
  - 3.2. Independent Fragmentation
  - 3.3. Cluster Fragmentation
  - 3.4. Other Fragmentation Approaches
  - 3.5. Particles and Their Decays
- 4. Our Experimental Knowledge
  - 4.1. Event Characterization Methods
  - 4.2. Event Shapes
  - 4.3. Multiplicities and Correlations
  - 4.4. Jet Type Separation
  - 4.5. String and Coherence Phenomena
- 5. Summary and Outlook

---

†lectures at the Cargèse Summer Institute on 'Z^0 Physics', Cargèse, France, August 14–24, 1990, and at the XVIII International Meeting on Fundamental Physics and XXI G.I.F.T. International Seminar on Theoretical Physics on 'Precision Tests of the Standard Model at High Energy Colliders', Santander, Spain, June 4–9, 1990

CERN-TH.5902/90
October 1990

1 Introduction

LEP has brought spectacular confirmation of the basic validity of the standard model, both in the electroweak and in the strong sector. Whereas tests of the electroweak model typically aim at very high precision, the QCD aspects are rather less under control. In particular, the fragmentation process has not yet been understood from first principles, but only in terms of vaguely QCD-inspired models, with many issues unsolved. Even in the large momentum transfer regime, where perturbative calculations can be used to describe jet production, the strong coupling constant α_S is large enough that yet uncalculated higher order corrections could well shift current results significantly. The status is reflected in these lectures, which contain a mixed bag of success stories and not yet resolved issues, but it should always be kept in mind that the underlying theory of QCD is not in question.

QCD is a non-Abelian gauge theory, with a well-defined Lagrangian, see e.g. [1]. Quarks appear in a colour triplet representation, and gluons in a colour octet one. There are three fundamental vertices in the theory: a quark-(antiquark-)gluon vertex, a three-gluon vertex and a four-gluon vertex. While the first is the analogue of the standard QED coupling of a charged particle to a photon, the latter two are absent in QED and reflect the non-Abelian structure of QCD. The four-gluon vertex appears only in higher orders, and does not have any major experimental consequences; for the renormalizability of the theory its presence is essential, however.

The theory contains one common coupling parameter, the strong coupling constant α_S. In the framework of the QCD renormalization group, α_S is found to be running with the momentum transfer scale Q^2. To first order, this is expressed by the relation

$$\alpha_S(Q^2) = \frac{12\pi}{(33 - 2n_f)\ln(Q^2/\Lambda^2)}, \tag{1}$$

where n_f gives the effective number of quarks, for e^+e^- annihilation normally taken to be 5 at the Z^0 scale, and Λ is a free dimensional parameter of the theory.

At short distances, which by the uncertainty principle corresponds to large momentum transfer scales, α_S is a reasonably small number. This is the region of 'asymptotic freedom', where quarks and gluons behave as almost free particles, and standard perturbation theory can be used to calculate their interactions. At large distances, on the other hand, the effective Q^2 scale is small and α_S becomes very large. Therefore the perturbative treatment in terms of quarks and gluons breaks down. Although it has not been fully proven mathematically, lattice QCD calculations give strong support to the concept of 'confinement', i.e. that quarks never appear as free particles, but are always confined inside colour singlet hadrons. The transition process, whereby the quarks and gluons turn into a set of hadrons, is called fragmentation or hadronization.

The structure of a typical multihadronic event in e^+e^- annihilation is shown in Fig. 1. A few introductory paragraphs, based on this figure, follow. A number of complications are here swept under the carpet, and only covered (if at all) in the subsequent, more detailed discussion.

In a first phase, an e^+e^- pair annihilates into a virtual γ/Z^0 state, which in its decay produces a primary quark-antiquark pair $q\bar{q}$. Before the annihilation, initial state QED bremsstrahlung may occur, so that the mass of the hadronic final state is reduced from the naive value. For the precision needed for Z^0 line shape studies, also higher order (loop) corrections to the basic graph are important. These aspects are covered e.g. in the LEP physics yellow book [2].

In the second phase, the initial $q\bar{q}$ pair may radiate gluons g, which in their turn may radiate. While the primary $q\bar{q}$ production is mainly given by electroweak perturbation theory, strong perturbation theory must be used to describe this second stage. The strong coupling constant being larger than the electroweak ones, the degree of accuracy is less, in particular for soft parton emission.

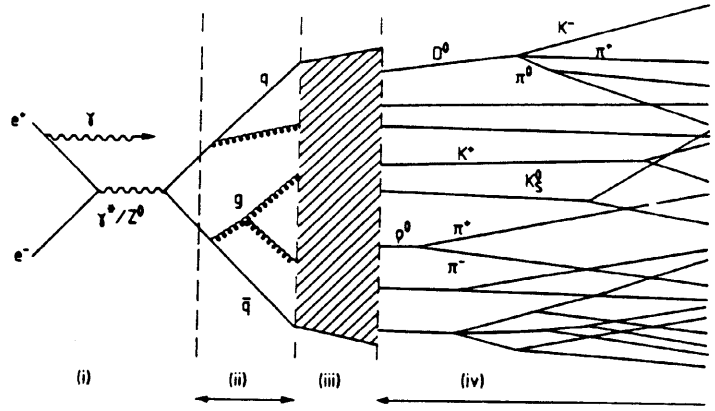

Figure 1: Schematic illustration of an e^+e^- annihilation event.

In the third phase, the coloured partons fragment into a number of colourless hadrons. Although we believe this process to be given by QCD, it is not perturbatively calculable, and therefore it is an area where phenomenological models have to be invoked.

In a fourth phase, unstable hadrons decay into the experimentally observable particles. This includes everything from $\pi^0 \to \gamma\gamma$ decays to long decay chains of charm and bottom hadrons. Whereas the qualitative features of these decays usually are well known, little quantitative understanding exists. Instead the main input here comes from experimentally determined branching ratios.

Given the complexity of the problem, purely analytical techniques are of limited usefulness for LEP physics studies. Instead the Monte Carlo simulation of complete hadronic events constitutes one of the main tools for improving our understanding of QCD at LEP. The use of Monte Carlo methods, i.e. the selection of variables according to rules which contain random numbers, is well suited to describe a Nature which is random in itself, and in addition allows the subdivision of a complex task into more manageable subtasks. In order to put the original theory or model on a computer, some compromises may be necessary, but on the other hand the Monte Carlo event generator approach makes it necessary to specify a number of details that often are dismissed cavalierly in purely analytical studies. It should still be recognized that the Monte Carlo approach, based as it is on a probabilistic description, in the end cannot be used to describe all subtle quantum mechanical effects [3], and that therefore analytical studies at times may be the only viable alternative.

A detailed review of existing QCD event generators is found in [3], from which part of the material in these lectures is taken, and to which we refer for all program details. The list of programs studied in the report is given in Table 1. The contents of these programs is classified according to the phases listed above, which also pretty much represent the general 'flow chart' of the programs. However, the hard interaction and initial state γ radiation aspects typically only correspond to less than 10% of the code (and the precision is nowhere near that of dedicated line shape programs) — most of the emphasis is put on the perturbative and fragmentation sections of the programs. Not all programs in Table 1 are equally ambitious, and in these lectures only a few will appear explicitly. Thus, essentially all LEP studies presented so far have been based on JETSET ('the Lund Monte Carlo') or HERWIG ('Marchesini-Webber').

The rapid variation of the electroweak cross-section around the Z^0 peak necessi-

Table 1: Physics components included in the programs covered in the LEP physics yellow book [3]. A '•' signifies that a task is handled in the program, a '+' that it is obtained by calling on another program (of the ones listed here), and a '-' that it is not considered at all. For some programs, the classification may not always be trivial, so this table should only be taken as a first indication. The symbols contain no grading on the quality of a program for a given task.

Program (comment)	Hard inter.	Initial γ rad.	Parton shower (or matrix el.)	Fragmentation	Decays
ARIADNE	+	+	•	+	+
CALTECH-II	•	-	•	•	•
COJETS	•	•	•	•	•
DPSJET (non-QCD)	-	-	•	•	-
EPOS (non-QCD)	•	-	•	•	•
EURODEC	-	-	-	•	•
HERWIG	•	-	•	•	•
JETSET ('Lund')	•	•	•	•	•
NLLJET	•	•	•	+	+
PARJET	•	-	•	•	•
TIPTOP (heavy ferm.)	•	•	-	+	+

tates special attention to fine details, like the effects of multiple soft photon initial state radiation. Programs written for use at lower energies (PETRA and PEP, say) can therefore in general not be taken over for LEP studies. In QCD the situation is quite different. The only significant consequences of the Z^0 peak for QCD studies are a somewhat changed primary quark composition and a different forward-backward quark production asymmetry. For the rest, QCD physics extrapolates smoothly from lower energies, such that the accumulated experience from PETRA, PEP and TRISTAN could be directly applied for LEP predictions. The LEP QCD event generators therefore are pretty much the same as those which have already seen heavy use at lower energies.

2 Perturbative QCD

The modelling of perturbative QCD is, together with the fragmentation modelling, the central objective of QCD studies. While the hard electroweak interaction provides a description of the production of a primary $q\bar{q}$ pair, the perturbative QCD description sets out to describe the emergence of multijet events. As the CM energy is increased, hard QCD emission is increasingly important, relative to fragmentation, in determining the event structure. At LEP, three- and four-jet event structures abound.

Two traditional approaches exist to the modelling of perturbative QCD. One is the matrix element method, in which Feynman diagrams are calculated, order by order. In principle, this is the correct approach, which takes into account exact kinematics, and the full interference and helicity structure. The only problem is that calculations become increasingly difficult in higher orders, in particular for the loop graphs. The calculations have therefore only been carried out, in full, up to $\mathcal{O}(\alpha_S^2)$. We have

indirect but strong evidence that, in fact, the emission of multiple soft gluons plays a significant rôle in building up the event structure at LEP energies, and this sets a limit to the applicability of matrix elements. However, the perturbative expansion by itself is more well behaved at LEP than at lower energies, due to the smaller α_S value, so inclusive measurements should yield more reliable results, e.g. in terms of α_S measurements [4].

The second possible approach is the parton shower one. Here an arbitrary number of branchings of one parton into two (or more) may be put together, to yield a description of multijet events, with no explicit upper limit on the number of partons involved. This is possible since the full matrix element expressions are not used, but only approximations derived by simplifying the kinematics, and the interference and helicity structure. Parton showers therefore are expected to give a good description of the substructure of jets, but in principle the shower approach has limited predictive power for the rate of well-separated jets (i.e. the 2/3/4/5-jet composition). In practice, shower programs may be patched up to describe the hard gluon emission region reasonably well. Nevertheless, the shower description is not optimal for absolute α_S determinations.

Thus the two approaches in many respects are complementary, and both have found use at LEP. However, because of its simplicity and flexibility of use, the parton shower option is generally the first choice, while the matrix elements one is mainly used for α_S determinations and three-gluon vertex studies. Obviously, the ultimate goal would be to have an approach where the best aspects of the two worlds are harmoniously married.

2.1 Matrix Elements

For the discussion in this section, we will use the word 'jet' also for properties on the partonic level, almost interchangeably with the word 'parton'. However, while a 'parton' is any quark or gluon appearing in the process description, a 'jet' is one or several nearby partons, lumped together according to some jet resolution criterion (see below). The 'true' number of partons in an event is thus an ill-defined concept (and may well be infinite), while the number of jets is unique (for a given jet definition).

2.1.1 First order matrix elements

The Born process $e^+e^- \to q\bar{q}$ is modified in first order QCD by the probability for the q or $\bar{q}$ to radiate a gluon, i.e. by the process $e^+e^- \to q\bar{q}g$, Fig. 2a. The matrix element is conveniently given in terms of scaled energy variables in the CM frame of the event, $x_1 = 2E_q/E_{CM}$, $x_2 = 2E_{\bar{q}}/E_{CM}$, and $x_3 = 2E_g/E_{CM}$, i.e. $x_1 + x_2 + x_3 = 2$. For massless quarks the matrix element reads [5]

$$\frac{1}{\sigma_0}\frac{d\sigma}{dx_1 dx_2} = \frac{\alpha_S}{2\pi} C_F \frac{x_1^2 + x_2^2}{(1-x_1)(1-x_2)}, \tag{2}$$

where σ_0 is the lowest order cross-section, $C_F = 4/3$ is the appropriate colour factor, and the kinematically allowed region is $0 \le x_i \le 1, i = 1,2,3$. The x_k variable for parton k is related to the invariant mass m_{ij} of the remaining two partons i and j by

$$y_{ij} \equiv \frac{m_{ij}^2}{E_{CM}^2} = 1 - x_k. \tag{3}$$

In order to separate two-jets from three-jets, it is useful to introduce jet resolution parameters, either (ϵ, δ) or y.

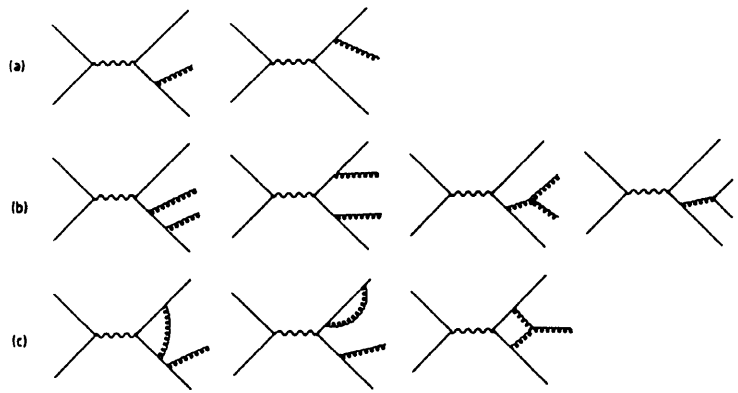

Figure 2: Feynman graphs for three- and four-jet production.
(a) The two graphs which contribute to three-jet production in first order.
(b) A few of the graphs which contribute to four-jet production (the ones left out can be obtained by symmetry).
(c) A few of the loop (vertex and propagator) graphs which contribute to three-jet production in second order.

- (ϵ, δ) : a three-parton configuration is called a two-jet event if $\min(x_i) < \epsilon$ or if $\min(\theta_{ij}) < \delta$ (where θ_{ij} is the angle between partons i and j in the CM frame of the event).
- y : a three-parton configuration is called a two-jet event if $\min(y_{ij}) = \min(m_{ij}^2/E_{CM}^2) < y$.

In the discussion which follows, we will mainly refer to the y cut case, since this is the simpler one.

The cross-section in eq. (2) diverges for $x_1 \to 1$ or $x_2 \to 1$ but, when first order propagator and vertex corrections are included, a corresponding singularity with opposite sign appears in the $q\bar{q}$ cross-section, so that the total continuum hadronic cross-section is finite, $\sigma_{tot}/\sigma_0 = 1 + \alpha_S/\pi$. In analytical studies, the average value of any well-behaved quantity $\mathcal{Q}$ can therefore be calculated as

$$\langle \mathcal{Q} \rangle = \frac{1}{\sigma_{tot}} \lim_{y \to 0} \left(\mathcal{Q}(2parton)\sigma_{2parton}(y) + \int_{y_{ij}>y} \mathcal{Q}(x_1, x_2) \frac{d\sigma_{3parton}}{dx_1 dx_2} dx_1 dx_2 \right), \qquad (4)$$

where any explicit y dependence disappears in the limit $y \to 0$. One should note that the hadronic Z^0 width receives a corresponding QCD correction factor as does σ_{tot} above: the net result is a reduction of the Z^0 peak cross-section.

In Monte Carlo programs, it is not possible to work with a negative total two-jet rate, and so it is necessary to introduce a fixed non-vanishing y cutoff in the three-jet phase-space. Experimentally, there is evidence for the need of a low y cutoff, i.e. a large three-jet rate. (Already at PETRA, this was apparent from the behaviour of the Energy-Energy Correlation Asymmetry [6].) For LEP applications, the recommended value is $y = 0.01$, which is about as far down as one can go and still retain a positive two-jet rate. With $\alpha_S = 0.12$, in full second order QCD, the $2:3:4$ jet composition is then approximately $11\% : 77\% : 12\%$.

A fixed cutoff in y corresponds to a minimum mass between any two jets that grows linearly with CM energy. For PETRA/PEP a cutoff at $y = 0.01$ (or slightly above, so as to keep a positive two-jet rate even for the somewhat higher α_S value at

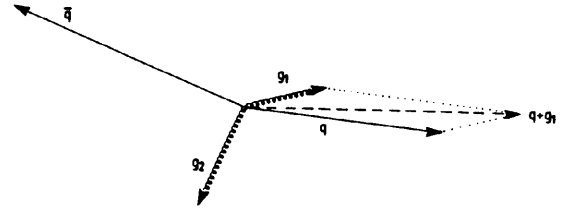

Figure 3: A four-parton event, with two nearby partons that are to be recombined. Construction of momentum sum $q+g_1$ is shown, but that gives a composite parton with non-zero mass.

lower energies) corresponds to a mass separation between jets of 3.5 GeV, at LEP it corresponds to 9 GeV. The nonperturbative fragmentation is expected to take over below a mass scale of around 1 GeV, independent of CM energy. As the energy is increased, there is therefore a widening soft gluon phase space region which cannot be simulated in a standard matrix elements based event generator. One may try to sum up the soft gluon effects into an effective energy-dependent fragmentation description, but this approach is fairly ugly and must eventually break down once sufficiently high energies are reached. As we shall see later, the Z^0 region is just at the borderline.

2.1.2 Second order matrix elements

Two new event types are added in second order QCD, $e^+e^- \to q\bar{q}gg$ and $e^+e^- \to q\bar{q}q'\bar{q}'$, Fig. 2b. Of the 12% four-jet rate quoted above, 11.5% is $q\bar{q}gg$ and only 0.5% $q\bar{q}q'\bar{q}'$.

The four-jet cross-section has been calculated by several groups [7,8,9,10], which agree on the result. The formulae are too lengthy to be quoted here. In one of the calculations [7], quark masses were explicitly included. The original calculations were for the pure γ exchange case; recently it has been pointed out [11] that an additional contribution to the $e^+e^- \to q\bar{q}q'\bar{q}'$ cross-section arises from the axial part of the Z^0. This term is not included in any QCD program so far, but fortunately it is finite and small.

As for the first order, a full second order calculation consists both of real parton emission terms and of vertex and propagator corrections, Fig. 2c. These modify the three-jet and two-jet cross-sections. Although there was some initial confusion, everybody eventually agreed on the size of the loop corrections [9,12,13]. In analytic calculations, the procedure of eq. (4), suitably expanded, can therefore be used unambiguously for any well-behaved variable.

For Monte Carlo event simulation, it is again necessary to impose some jet resolution criteria. This means that four-parton events which fail the four-jet cuts should be reassigned either to the three-jet or to the two-jet event class. It is this area which has caused quite a lot of confusion in the past [14]. The reasons for the confusion are well understood by now, but this does not mean we have reached agreement on a unique procedure to resolve the issue. Most likely, agreement will never be reached, since indeed there are ambiguous points in the procedure, related to uncertainties on the theoretical side. This is illustrated in the following paragraphs.

For the y-cut case, any two partons with an invariant mass $m_{ij}^2 < yE_{cm}^2$ should be recombined into one. If the four-momenta are simply added, Fig. 3, the sum will correspond to a parton with a positive mass, namely the original m_{ij}. The loop corrections are given in terms of final massless partons, however. In order to perform the (partial) cancellation between the four-parton real and the three-parton virtual contributions, it is therefore necessary to get rid of the bothersome mass. Several

procedures have been proposed; the following two are probably the most frequently used ones.

- The $\overline{p}$ recombination scheme: keep the constructed three-momentum sum $\overline{p}_{ij} = \overline{p}_i + \overline{p}_j$ (in the CM frame of the event), and redefine the energy of the recombined parton as being $E_{ij} = |\overline{p}_i + \overline{p}_j|$. Since $E_{ij} < E_i + E_j$, the total CM energy of the event has been reduced, which can be compensated by rescaling all the four-momenta in the event by a common factor.
- The E recombination scheme: require $E_{ij} = E_i + E_j$. The three variables x_1, x_2 and x_3 are then easily obtained, but the three-momenta have to be modified in a non-trivial manner to keep momentum conserved.

The E scheme obviously gives more energy to the recombined jet than does the $\overline{p}$ one. Since the typical situation is that the recombined jet still is the lowest-energy one (two soft gluons recombined into a medium soft one), the E scheme gives more three-jetlike topologies than the $\overline{p}$ one, and so has a larger (i.e. more positive) second order correction to the three-jet rate.

The total number of different recombination schemes proposed is fairly large, and so is the list of different parametrizations of the second order three-jet rate. Fig. 4 shows a comparison of some of these parametrizations [3]. (Further recent comparisons between schemes may be found in [4,15].) While the GKS curve is known to be wrong (in the sense that it is based on a number of analytical approximations we now know are unacceptably crude), there is enough of a spread between the other ones. Experimental α_S determinations are typically based on the shape of the thrust distribution, and are thus particularly sensitive to the region $T < 0.85$. Here, however, four-jets give a non-negligible contribution (actually the ratio becomes infinite at $T = 2/3$, since three-jet phase-space vanishes at that point, while four-jets may have $T < 2/3$). The net effect is thus that the uncertainty in the value of the thrust distribution is nowhere larger than $\pm 10\%$, based on the generators above. This gives some feeling for what 'theory systematic error' need to be assigned to any α_S determination, just from the matrix element point of view. Additional uncertainties come from higher orders, from fragmentation, from experimental errors, and so on.

If the situation is complicated enough for the y cut, it is even worse for the (ϵ, δ) alternative. Separate recipes need to be specified for what to do when a parton fails the ϵ cut, when a pair fails the δ cut, and when both happen in the same event. In particular, for the ϵ cut, one could either discard the soft parton outright, or choose between several possible recombination algorithms. The spread in effective three-jet rate, i.e. in terms of α_S values found for given data, has therefore always been larger in the (ϵ, δ) alternative. None of the algorithms in use today are based on (ϵ, δ) cuts.

In a complete second order description, consistency requires the use of the second order expression for α_S. Several alternative forms exist, which only differ by terms nominally of order α_S^3. The standard proposed by the Particle Data Group [16] is

$$\alpha_S(Q^2) = \frac{12\pi}{(33-2n_f)\ln(Q^2/\Lambda^2)}\left[1 - 6\frac{153-19n_f}{(33-2n_f)^2}\frac{\ln(\ln(Q^2/\Lambda^2))}{\ln(Q^2/\Lambda^2)}\right]. \tag{5}$$

Further, the total continuum hadronic cross-section is [17]

$$\frac{\sigma_{tot}}{\sigma_0} = 1 + \frac{\alpha_S}{\pi} + (1.986 - 0.115n_f)\left(\frac{\alpha_S}{\pi}\right)^2. \tag{6}$$

It should be mentioned that σ_{tot} was calculated to third order a few years ago [18]. This calculation gave a surprisingly large third order term. The authors have now found an error in that calculation, but have not yet provided a corrected result. Currently, σ_{tot} should therefore be considered to be known only to second order.

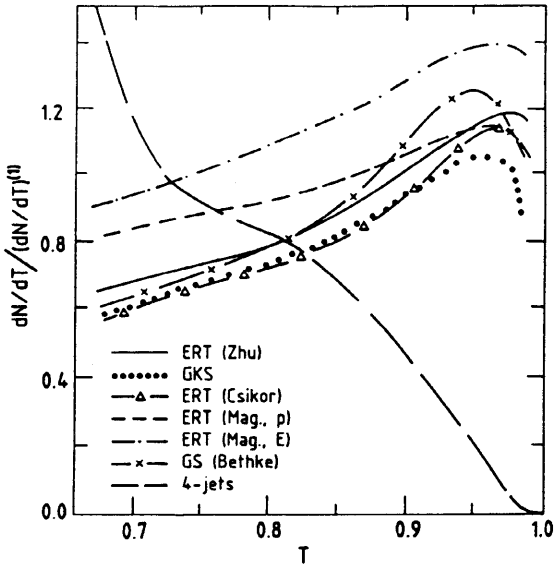

Figure 4: Full second order three-jet thrust distribution, normalized to the first order one, for $\alpha_S = 0.12$ and $y = 0.01$. Also shown is the four-jet thrust distribution, normalized the same way.

2.1.3 Optimized perturbation theory

The second order corrections to the three-jet rate are large. It is therefore not unreasonable to expect large third order corrections to the four-jet rate. Indeed, the experimental four-jet rate is much larger than second order predicts (also when fragmentation effects have been taken into account), if α_S is determined based on the three-jet rate [6,19,20,21].

The only consistent way to resolve this issue is to go ahead and calculate the full next order. This is a tough task, however, so people have looked at possible shortcuts. For example, one can try to minimize the higher order contributions by a suitable choice of the renormalization scale — 'optimized perturbation theory'. This is equivalent to a different choice for the Q^2 scale in α_S, a scale which is not unambiguous anyway. Indeed the standard value $Q^2 = s = E_{CM}^2$ ($= M_Z^2$ at LEP) is larger than the natural physical scale of gluon emission in events, given that most gluons are fairly soft. One could therefore pick another scale, $Q'^2 = fs$, with $f < 1$. Since α_S is increased by a reduction of the Q^2 scale, the $\mathcal{O}(\alpha_S)$ three-jet rate would then be increased, and so would the number of four-parton events, including those which collapse into three-jet ones. The loop corrections depend on the Q^2 scale, however, and compensate the changes above by giving a larger negative contribution to the three-jet rate.

The transformation to a different scale can be done easily as follows. Suppose that the three-jet rate R_3 (differential or integrated over some region of phase space) is given in a certain renormalization scheme and for a scale $Q^2 = s$

$$R_3 = r_1\alpha_S + r_2\alpha_S^2 + \mathcal{O}(\alpha_S^3), \tag{7}$$

with

$$\alpha_S \equiv \alpha_S(Q^2) = \frac{12\pi}{(33-2n_f)\ln(Q^2/\Lambda^2)} = \frac{1}{b\ln(Q^2/\Lambda^2)} \tag{8}$$

(in the formulae in this section we use the first order α_S expression for simplicity; to our required level of approximation an inclusion of the full second order expressions changes nothing in the following argumentation).

When the coupling is chosen at a different scale, $Q'^2 = fQ^2$, this corresponds to a change of the α_S value according to

$$\begin{aligned}
\alpha'_S &\equiv \alpha_S(Q'^2) = \frac{1}{b\ln(fQ^2/\Lambda^2)} = \frac{1}{b\left[\ln(Q^2/\Lambda^2)+\ln f\right]} \\
&= \frac{1}{b\ln(Q^2/\Lambda^2)}\,\frac{1}{1+\frac{\ln f}{\ln(Q^2/\Lambda^2)}} = \alpha_S\left(1-\frac{\ln f}{\ln(Q^2/\Lambda^2)}+\cdots\right) \\
&= \alpha_S\left(1-b\alpha_S\ln f+\cdots\right) = \alpha_S - b\alpha_S^2\ln f + \mathcal{O}(\alpha_S^3). \qquad (9)
\end{aligned}$$

The expression for the three-jet rate reads

$$\begin{aligned}
R'_3 &= r'_1\alpha'_S + r'_2\alpha'^2_S + \mathcal{O}(\alpha'^3_S) = r'_1(\alpha_S - b\alpha_S^2\ln f+\cdots) + r'_2(\alpha_S+\cdots)^2 + \mathcal{O}(\alpha_S^3) \\
&= r'_1\alpha_S + (r'_2 - r'_1 b\ln f)\alpha_S^2 + \mathcal{O}(\alpha_S^3). \qquad (10)
\end{aligned}$$

The concept of the renormalization group asserts that, if a physical quantity like the three-jet rate R_3 is calculated to infinite order, no dependence can remain on the original choice of the expansion parameter α_S. If calculated to infinite order, one must therefore have $R'_3 \equiv R_3$. Thus, in particular, if R_3 and R'_3 are given in terms of power series in the same α_S parameter, the coefficients must be the same, order by order (since formally α_S can be varied continuously, independently of the f choice, by a change of the CM energy). Comparing eqs. (7) and (10) one concludes that

$$\begin{aligned}
r'_1 &= r_1, \\
r'_2 &= r_2 + r_1 b\ln f, \qquad (11)
\end{aligned}$$

i.e.

$$R'_3 = r_1\alpha'_S + (r_2 + r_1 b\ln f)\alpha'^2_S + \mathcal{O}(\alpha'^3_S). \qquad (12)$$

The net effect is to make the physical three-jet rate less dependent on the choice of scale Q'^2, i.e. f, in α_S: if f is made smaller (keeping Λ fix), the effective parameter α'_S becomes larger, but simultaneously r'_2 is made smaller, such that R'_3 is not changed very much. That R'_3 is not completely independent of f is only a consequence of the approximations made in relating α'_S to α_S; the differences are formally of $\mathcal{O}(\alpha_S^3)$, but may become large when f is varied over a large range. When fitting to an experimentally measured three-jet rate, such variations are reflected in a necessity to use slightly different Λ values for different f:s.

Since only the Born term has been calculated for four-jets, the four-jet rate is directly proportional to α_S^2. As f is decreased (again for fixed Λ), the increase in α'_S therefore directly leads to an enhanced four-jet rate. It is exactly this feature that makes it possible to solve the mystery of the lacking four-jets in the older standard matrix element implementations, which used $f = 1$.

While the experimental motivation for considering optimized perturbation theory in e^+e^- came from the problems with the four-jet rate, in fact a number of theorists have earlier proposed recipes for selecting which scale to use for a process, if the one loop corrections to the Born term cross-section are already available. These recipes go by names such as PMS (principle of minimal sensitivity) [22], FAC (fastest apparent convergence) [23], or BLM [24]. While different in detail, they have in common that, the larger the relative size of the second order term (i.e. the ratio r_2/r_1), the smaller the preferred scale. Therefore these schemes all strongly suggest the correct scale to be smaller than the naive $Q^2 = M_Z^2$ one. Also on physical grounds it can be argued that, reasonably, the scale for the emission of a gluon should be related to the kinematics

of this emission, and thus be smaller than M_Z (a more precise statement will come in the parton shower section). However, only a full higher order calculation would in the end tell whether a particular choice is favoured or not.

A number of α_S determinations have now been presented by the LEP groups [25]. With $f = 1$, typically one obtains $\alpha_S(M_Z^2) \approx 0.12$, or $\Lambda \approx 0.2$ GeV. If f is varied over a wide range, down to $f = 0.001$, say, Λ is found to be somewhere between 0.1 and 0.2 GeV. Plugging this Λ range into eq. (5), the LEP collaborations quote $\alpha_S(M_Z^2) \approx 0.11$—$0.12$, and conclude that this value is rather independent of the choice of f. Unfortunately, the claimed constancy of α_S may lead the unwary reader astray. For a proper understanding, it is important to make a distinction between $\alpha_S(fM_Z^2)$ and $\alpha_S(M_Z^2)$ in studies where an $f < 1$ is used. The $\alpha_S(fM_Z^2)$ value is α_S as actually extracted from the experimental data, e.g. in terms of jet rates or the Energy-Energy Correlation Asymmetry. This α_S typically is larger the smaller the f chosen, and may vary significantly: with $f = 0.001$ and $\Lambda = 0.1$ GeV, $\alpha_S(fM_Z^2) \approx 0.20$. It is only if the widely different $\alpha_S(fM_Z^2)$ values , determined for a wide range of f values, are evolved up to a common scale, M_Z^2, that the small $\alpha_S(M_Z^2)$ range noted above is obtained. The small range thus simply reflects the stability of the Λ value under variations of the choice of optimized scale. This aspect would not readily be appreciated by just quoting $\Lambda \approx 0.1$–0.2 GeV: since Λ only enters logarithmically into α_S, and therefore into any experimental observable, a factor 2 uncertainty would look more than it really is. In summary: the experimentally determined α_S value strongly depends on what optimized scale is picked, but the Λ value that is extracted remains fairly stable, as reflected in the small range of α_S values at the common scale M_Z^2.

Actually it should come as no surprise that the use of optimized perturbation theory is related to the use of a higher $\alpha_S(fM_Z^2)$ value, at least not if we remember the original motivation of pushing up the theoretical four-jet rate to the experimental level. Since this rate, to the order we have available, is directly proportional to α_S^2 and nothing else, obviously we would not be helped if optimized perturbation theory did not allow us to make α_S bigger (compared to $f = 1$), while still keeping the three-jet rate unchanged. Put this way, optimized perturbation theory could also be considered as a consistent scheme to decouple the descriptions of three-jet and four-jet production: in general, for an α_S adjusted to get the four-jet rate right, it is afterwards possible to find an f such that also the three-jet rate is well described. It is amusing to note that a pure first order fit to LEP data would give $\alpha_S \approx 0.18$, which then is reduced, for the three-jet rate, by second order contributions. It is therefore not a vain hope that, once third order corrections are included fully, the α_S needed for the four-jet rate will drop to around 0.12.

The appearance of an α_S value as high as 0.20 should not lead anybody to fear that QCD corrections to the total hadronic width of the Z^0 have a corresponding uncertainty: as was the case with the three-jet rate above, as soon as an $f < 1$ is used, such that the first order contribution to the width is increased, a compensating term automatically appears in the second order contribution, such that the total hadronic width is fairly insensitive to the choice of Q^2 scale. Let us work this out in a general case.

Consider two measures C and D, each with its expansion in terms of $\alpha_S = \alpha_S(Q^2)$,

$$\begin{aligned}
C &= c_0 + c_1\alpha_S + c_2\alpha_S^2, \\
D &= d_0 + d_1\alpha_S + d_2\alpha_S^2. \qquad (13)
\end{aligned}$$

The same derivation that gave eq. (12) now gives

$$\begin{aligned}
C' &= c_0 + c_1(\alpha'_S + b\ln f\alpha'^2_S) + c_2\alpha'^2_S, \\
D' &= d_0 + d_1(\alpha'_S + b\ln f\alpha'^2_S) + d_2\alpha'^2_S, \qquad (14)
\end{aligned}$$

at another scale $Q'^2 = fQ^2$. If the quantity C is used for defining the α_S value as a

function of the f scale then, by definition, $C' = C$. This implies that

$$\alpha_S' + b \ln f \alpha_S'^2 = \alpha_S - \frac{c_2}{c_1}(\alpha_S'^2 - \alpha_S^2). \tag{15}$$

If this is plugged into the expression for D', one obtains

$$D' = D + d_1 \left(\frac{d_2}{d_1} - \frac{c_2}{c_1} \right) \left(\alpha_S'^2 - \alpha_S^2 \right). \tag{16}$$

Note that any change in D appears only in second order in α_S.

The QCD corrections to the Z^0 hadronic width, which have the same form as the corrections to the continuum hadronic cross-sections, eq. (6), are characterized by a small second order coefficient, while typical event measures have a much larger (positive) ratio of second to first order coefficients. Therefore the tendency would be towards a smaller Γ_Z if optimized perturbation theory is used, with α_S' determined by event measures such as thrust or the multi-jet rate at the same optimized Q'^2 scale as is to be used for the hadronic width. However, it should be noted that the different ratios of second to first order coefficients for Γ_Z and typical event measures also implies different theoretically preferred optimized scales. For Γ_Z the scale should therefore be closer to M_Z^2, i.e. it is not motivated to consider values down to $f = 0.001$, as has been done in jet rate studies. Further, while eq. (16) gives a transparent description of the variation of an experimental quantity with the f parameter, it may not be the most convenient recipe for experimental studies.

Given the current large use of optimized scales, it is maybe appropriate to end this section with a warning. The second order corrections to the three-jet rate (i.e. the coefficient r_2) is positive in most regions of the three-jet phase space, but not everywhere. One region where it is negative is when the q and $\overline{q}$ are fairly close in phase space: since the q and $\overline{q}$ are in a relative colour octet (together with the colour octet gluon they have to make up a colour singlet), the colour force between them is repulsive, which translates into a negative loop correction [26]. Another region is where the gluon is very close either to the q or $\overline{q}$, and the first loop correction is partly related to the eventual buildup of a Sudakov form factor (see section 2.2.2). While regions with a negative differential first+second order three-jet rate can exist already for the simple choice $Q^2 = E_{CM}^2$, they become larger as smaller scales are used, simply because the relative importance of the second order terms to the three-jet rate becomes larger. Thus the total theoretical three-jet rates computed for small f values are positive only because kinematical variables have been integrated out, so that positive and negative regions have cancelled — a not very satisfactory state of affairs. This points the way towards further potentially necessary 'improvements' of the current treatment of three-jets, such as exponentiation of some of the terms into a Sudakov form factor (which, as a by-product, would also make it possible to use smaller y cut values).

2.1.4 Higher order matrix elements

A few years ago, three groups calculated the five-jet Born cross-sections [27,28]. This is certainly impressive, and could be useful for specific applications. So far, these formulae have not found wide spread use, for a number of reasons. First, the formulae are lengthy; generation of unweighted events is therefore slow. Second, the actual rate of five-jet production is small, even when increased by the use of an optimized scale as described above. Third, inclusion of five-jets will not help at all for α_S determinations so long as loop corrections to the same order are not available.

The techniques developed not only make it possible to calculate five-jet matrix elements, but also processes of the type $q\overline{q}(ng), n \geq 0$, i.e. with an arbitrary number

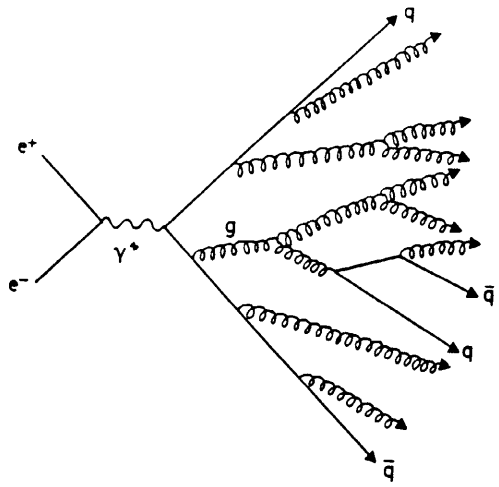

Figure 5: Schematic picture of parton shower evolution in e^+e^- events.

of gluons [28]. Matrix element evaluation is slow for many gluons, but simpler approximate expressions exist [29], which preserve the full pole structure, and numerically seem to agree with the exact results on the 10% level. These could come in very handy for topological studies.

2.2 Parton Showers

The parton shower picture is derived within the framework of the leading logarithm approximation, the LLA. In this picture, only the leading terms in the perturbative expansion are kept and, where need be, resummed. Subleading corrections, which are down in order by factors of $\ln Q^2$ or $\ln z$ ($\ln(1-z)$), or by powers of $1/Q^2$, are thus neglected. Different schemes have been devised for taking into account some subleading corrections; they appear under names like MLLA (M for modified) or NLLA (N for next-to-) [30]. The overall theoretical picture is rather encouraging: there is reason to believe that neglected subleading effects are small, and the predictive power of this approach is increasing year by year.

Phenomenologically, the main reason for the LLA success is the ability to formulate LLA in terms of a probabilistic picture, suitable for event generation. The approach is based on simplifications in kinematical variables, however, so the predictive power for hard, wide-angle parton emission remains limited.

2.2.1 The evolution equations

Most parton shower algorithms are based on an iterative use of the basic branchings $q \to qg$, $g \to gg$, and $g \to q\overline{q}$, Fig. 5. A probabilistic picture is used to describe these branchings, as follows.

The probability $\mathcal{P}$ that a branching $a \to bc$ will take place during a small change $dt = dQ_{evol}^2/Q_{evol}^2$ of the evolution parameter $t = \ln(Q_{evol}^2/\Lambda^2)$ is given by the Altarelli-Parisi equations [31]

$$\frac{d\mathcal{P}_{a\to bc}}{dt} = \int dz \frac{\alpha_S(Q^2)}{2\pi} P_{a\to bc}(z). \tag{17}$$

For gluons it is necessary to sum over all allowed final state flavour combinations b and c to obtain the total branching probability. The $P_{a\to bc}(z)$ are the Altarelli-Parisi splitting kernels

$$\begin{aligned} P_{q\to qg}(z) &= C_F\frac{1+z^2}{1-z}, \\ P_{g\to gg}(z) &= N_C\frac{(1-z(1-z))^2}{z(1-z)}, \\ P_{g\to q\bar{q}}(z) &= T_R(z^2+(1-z)^2), \end{aligned} \tag{18}$$

with $C_F = 4/3$, $N_C = 3$, and $T_R = n_f/2$, i.e. T_R receives a contribution of $1/2$ for each allowed $q\bar{q}$ flavour. The z variable specifies the sharing of four-momentum between the daughters, with daughter b taking fraction z and c taking $1-z$. Usually the first order α_S is used, eq. (1); as we shall see, the Q^2 scale of α_S need not agree with the evolution scale Q^2_{evol}.

Persons familiar with analytical calculations may wonder why the '+ prescriptions' and $\delta(1-z)$ terms of the splitting kernels in eq. (18) are missing. These complications fulfil the task of ensuring flavour and energy conservation in the analytical equations. The corresponding problem is solved trivially in Monte Carlo programs, where the shower evolution is traced in detail, and flavour and four-momentum are conserved at each branching. The legacy left is the need to introduce a cutoff on the range of the z integral in the Altarelli-Parisi equations, so as to avoid the singular regions corresponding to excessive production of very soft gluons. Typically, this is achieved by introducing an effective (fictitious) gluon mass (in programs usually denoted by Q_0 or $Q_0/2$).

Also note that $P_{g\to gg}(z)$ is given here with a factor N_C in front, while it is sometimes shown with $2N_C$. The difference of a factor of two comes from either considering the number of gluons that branch or the number of gluons that are produced.

2.2.2 The Sudakov form factor

Starting at the maximum allowed virtuality t_{max} for parton a, the t parameter may be successively degraded. This does not mean that an individual parton runs through a range of t values: each parton in the end is associated with a fixed t value, and the evolution procedure is just a way of picking that value. It is only the ensemble of partons in many events that evolve continuously with t, cf. the concept of structure functions. The probability that no branching occurs during a small range of t values, δt, is given by $(1-\delta t\, d\mathcal{P}/dt)$. When summed over many small intervals, the no-emission probability exponentiates

$$\mathcal{P}_{no-emission}(t_{max},t) = \exp\left(-\int_t^{t_{max}} dt' \frac{d\mathcal{P}_{a\to bc}}{dt'}\right). \tag{19}$$

Thus the actual probability for a branching of a given t is the naive probability, eq. (17), multiplied by the probability that a branching has not already taken place, eq. (19). This is nothing but the exponential decay law of radioactive decays, with a t-dependent decay probability.

It is customary to introduce the Sudakov form factor, i.e. the probability that a parton starting from a maximum virtuality t will reach the fixed lower cutoff t_{min} (related to the effective gluon mass Q_0) without branching

$$S_a(t) = \exp\left(-\int_{t_{min}}^{t} dt' \int_{z_{min}(t')}^{z_{max}(t')} dz \frac{\alpha_S(Q'^2)}{2\pi} P_{a\to bc}(z)\right). \tag{20}$$

The no-emission probability above is then just $S_a(t_{max})/S_a(t)$.

Once the branching of parton a has been selected, the products b and c may be allowed to branch in their turn, and so on, giving a treelike structure. The branching of a given parton is stopped whenever the evolution parameter is below t_{min}.

2.2.3 Coherence

Very valuable input for model builders is provided by the theoretical studies of corrections beyond leading log, like coherence effects [32,26]. The latter come in two kinds.

- The intrajet coherence phenomenon is responsible for a decrease of the amount of soft gluon emission inside jets. It has been shown that an ordering in terms of a decreasing emission angle takes into account the bulk of soft gluon interference effects. Algorithms which contain angular ordering are loosely said to produce coherent showers, while those without generate conventional ones.
- The interjet coherence phenomenon, responsible for the flow of particles in between jets, with constructive or destructive interference depending on colour configuration ('colour drag phenomena'), cf. [26]. This form of coherence is not just a direct consequence of the ordering of (polar) emission angles mentioned above, but also requires that azimuthal angles of branchings be properly distributed.

The coherence phenomenon is known already from QED. One manifestation is the Chudakov effect [33], discovered in the study of high energy cosmic γ rays impinging on a nuclear target. If a γ is converted into a highly collinear e^+e^- pair inside the emulsion, the e^+ and e^- in their travel through the emulsion ionize atoms and thereby produce blackening. However, near the conversion point the blackening is small: the e^+ and e^- then still are close together, such that an atom passed by the pair does not resolve the individual charges of the e^+ and the e^-, but only feels a net charge close to zero. Only later, when the e^+ and e^- are separated by more than a typical atomic radius, are the two able to ionize independently of each other.

The situation is similar in QCD, but is further extended, since now also gluons carry colour. For example, in a branching $q_0 \to qg$ the q and g share a colour-anticolour pair, and so the q and g can not emit further gluons incoherently. Again the net effect is to reduce the amount of soft gluon emission: since a soft gluon (emitted at large angles) corresponds to a large (transverse) wavelength, the soft gluon is unable to resolve the separate colour charges of the q and the g, and only feels the net charge carried by the q_0. Such a soft gluon g' (in the region $\theta_{q_0g'} > \theta_{qg}$) could therefore be thought of as being emitted by the q_0 rather than by the q–g system. If one only considers emission which should be associated with the q or the g, to a good approximation, there is a complete destructive interference in the regions of non-decreasing opening angles, while partons radiate independently of each other inside the regions of decreasing opening angles ($\theta_{qg'} < \theta_{qg}$ and $\theta_{gg'} < \theta_{qg}$), once azimuthal angles are averaged over. The details of the colour interference pattern are reflected in non-uniform azimuthal emission probabilities.

Another effect beyond the predictability of leading logs concerns the scale choice in α_S. Here theoretical studies of loop corrections [30] strongly suggest the use of a scale $Q^2 = z(1-z)m_a^2 \approx p_T^2$, i.e. the scale is set by the transverse momentum of a branching, rather than by the mass of the decaying parton, as might naively have been expected. Specifically, what happens if one uses the m^2 scale is that the second order calculation of splitting kernels gives large terms, which are proportional to the first order splitting kernels times factors of $\alpha_S \ln z$ and $\alpha_S \ln(1-z)$. With the modified scale choice $z(1-z)m^2$ it is possible to absorb these large terms into the (nominally) lowest order expressions, cf. eq. (9).

2.2.4 Shower programs

A wide selection of shower algorithms have been developed, see [3], which mainly differ in the interpretation of the variables t (or Q^2_{evol}), Q^2 and z. Many of the variations formally are of a subleading character, and therefore are not constrained by theoretical leading log analyses, while others imply quite different physics, at least at higher energies.

While z generically expresses the sharing of energy and momentum between the two daughters, the exact definition varies from program to program. It is possible to define z in terms of energy E, in terms of light-cone momentum $E + p_L$, in terms of $E + |\vec{p}|$, or in terms of some other combination of energy and momentum. The definition chosen affects the allowed region of z values, i.e. the $z_{min}(t)$ and $z_{max}(t)$ functions of eq. (20). The introduction of angular ordering actually constrains the allowed z range, compared to the kinematically allowed one. Since the details of the z interpretation are most significant at low z values, angular ordering as a 'fringe benefit' introduces a reduced dependence on the z choice made.

One should note that none of the z definitions given above are fully Lorentz covariant, and hence neither are most shower algorithms. From a theoretical point of view, this is related to the need to fix a gauge before the branching probabilities can be evaluated (it is e.g. possible to have an algorithm where only one of the initial two partons radiate). The general belief is that the breaking of Lorentz covariance here is a rather minor point, with no experimentally observable consequences ...

The best known coherent shower algorithm is probably the Marchesini-Webber (HERWIG) one [34], where angular ordering is built in from the onset. Here $Q^2_{evol} = E^2\xi$, with $\xi \approx 1 - \cos\theta$. E is the energy of the branching parton and θ the opening angle between its decay products. Since E is fix, a decrease of Q^2_{evol} is equivalent to a decrease of the opening angle in the branching. Once the decay angular variable ξ_a is known, the maximum Q^2_{evol} scale of the two daughters is now given by $E_b^2\xi_a$ and $E_c^2\xi_a$, respectively, because of the requirement of angular ordering. These daughters may be degraded in their turn, to find $\xi_b < \xi_a$ and $\xi_c < \xi_a$, etc.

The Marchesini-Webber algorithm is different from others in several respects. One is that parton masses are not defined during the evolution stage. Only afterwards are parton masses constructed from the final on-shell partons backwards to the shower initiator, by using the opening angle variable, and only after that is the actual kinematics of the shower found. Most other programs construct the kinematics in parallel with the shower evolution proper. Another difference is that the Marchesini-Webber algorithm makes use of an evolution variable which explicitly involves angles, and which thereby automatically incorporates angular ordering.

In many other algorithms, such as the one implemented in JETSET [35], the evolution variable is defined to be $Q^2_{evol} = m_a^2$, i.e. the mass of the decaying parton. This means that angular ordering is not included automatically, but must be imposed as an additional constraint on the combination of m^2 and z values which are allowed for a particular branching, given the m^2 and z values of the preceding branching.

Since showers are so important for phenomenological studies at higher energies, a steady evolution is taking place in the field. Three main approaches can be distinguished for this improvement. One is to refine the standard (modified) leading log picture as such, by including further corrections and effects. Another is to go beyond leading log, and to include also higher order effects. The third is to strive for an alternative (but equivalent) formulation of the shower process, where a number of non-trivial effects are included from the beginning. A few words about each of these.

One way to improve on the basic picture is to include non-isotropic azimuthal angles. This is particularly well explored by HERWIG, in which the following three sources of anisotropy are included:

- Gluon polarization, leading to a correlation between the production and decay planes of a gluon.
- Gluon polarization, also giving correlations between non-adjacent branchings, i.e. of the 'Bell inequality' type [36].
- Soft gluon interference, related to the fact that the soft gluon emission probability is actually obtained by summing emission amplitudes from a number of separate hard partons.

Another possible improvement, found e.g. in JETSET, is to constrain the first branchings of the shower to agree with the explicit three-jet matrix element form. This is an attempt to modify the shower formalism in the region where the kinematical approximations involved are known to be least reliable, while still preserving concepts of the LLA such as the Sudakov form factor and the $Q^2 \approx p_T^2$ argument in α_S.

As the name suggests, NLLjet [37] is a program which tries to go beyond leading order, to Next-to-Leading-Logs. The most apparent consequence is the introduction of $1 \to 3$ parton branchings: $q \to qgg, q \to qq'\bar{q}', g \to ggg$, and $g \to gq\bar{q}$. Also the ordinary $1 \to 2$ branchings are modified, in analogy with the second order three-jet matrix element modifications. Since loop graphs are explicitly involved in calculating the corrections, the Q^2 scale definition is under better control. From that point of view, NLLjet should be superior for Λ determinations. Unfortunately, as for leading logs, the whole approach is really only valid for collinear kinematics. A number of additional assumptions are needed for extrapolations to the interesting region of well separated jets.

An alternative to parton shower algorithms is the dipole formulation of ARIADNE [38], suggested by the Leningrad group [39], and studied in detail by the Lund people. The picture is based on identifying the string pieces between partons with colour dipoles or colour antennae, so that the emission of a gluon corresponds to the breaking of a dipole into two. This breaking is simple and well-defined in the rest frame of a dipole, and yet it automatically includes angular ordering and non-trivial azimuthal effects when the boost back to the overall CM frame is taken into account. The picture has a number of appealing features, e.g. an explicitly Lorentz covariant formulation, and may well come closer to describing nature as it really is than do the other algorithms. This does not mean it is a unique recipe. While angular ordering is built in, the transverse momentum of a dipole branching is a priori not required to be smaller than the p_T of the branching in which it was produced; the model is rather sensitive to what is assumed on this count. Additional degrees of freedom in branchings come from the angular orientation of daughter dipoles with respect to the mother one.

2.3 Testing QCD

The theory of QCD seems to be in excellent shape. This in part reflects on the quality of QCD, but also on the difficulty to construct a consistent alternative that is not already excluded by data. We also know of no good way to slightly 'deform' QCD, such that only subtle differences would remain in experimental observables. This in contrast to the electroweak sector, where e.g. the introduction of a Z' could be used to shift slightly the predictions for the ordinary Z.

Two toy models have been used frequently, just so as to have something to compare with QCD. One is a scalar gluon model, i.e. where the gluon has spin 0 rather than 1. This leads to observable differences already on the three-jet level [5,40]:

$$\frac{1}{\sigma_0}\frac{d\sigma}{dx_1 dx_2} \propto \frac{x_3^2}{(1-x_1)(1-x_2)}, \tag{21}$$

to be contrasted with eq. (2). PETRA three-jet data were used to exclude this possibility [41].

A somewhat more interesting alternative is the Abelian gluon model, where the gluon has spin 1 but does not carry any colour, i.e. where QCD is pretty much like

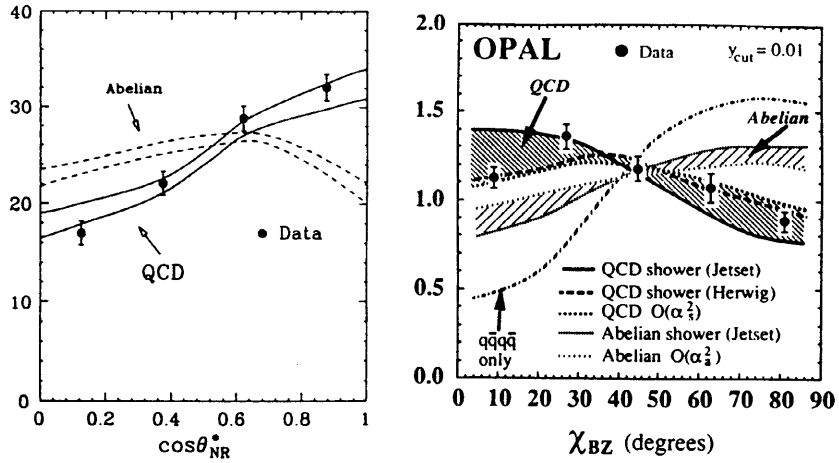

Figure 6: Examples of angular distributions in two of the four-jet angles used to distinguish between QCD and the Abelian model. Left the NR^* variable measured with L3 [47], right the BZ one of OPAL [46].

ordinary QED. There are a number of reasons why this model is already counterindicated, ranging from the absence of confinement and the incorrect running of α_S [42] in the model, to the contradiction with Υ decay [43] and $p\bar{p}$ [44] data. The differential three-jet rate is the same as for ordinary QCD (modulo the different running of α_S), so tests based on angular distributions of jets have to be performed by looking at four-jet events. The changes here can be summarized as follows.

- The colour factor C_F, related to the bremsstrahlung of a gluon off a quark, is changed from 4/3 in ordinary QCD to 1 in the Abelian model; effectively this change is absorbed in the necessity to tune α_S to data anyway. The rate of four-jets from double gluon bremsstrahlung therefore remains unchanged.
- The colour factor N_C is changed from 3 to 0; the three-gluon vertex $g \to gg$ is thus absent in the Abelian theory, just like there is no vertex $\gamma \to \gamma\gamma$ in QED.
- The colour factor T_R is changed from $n_f/2$ to $3n_f$, i.e. the branchings $g \to q\bar{q}$ are greatly enhanced. For a $y = 0.01$ cutoff, the $q\bar{q}q'\bar{q}'$ fraction of all four-jets is increased from 4.7% in QCD to 31% in the Abelian model, something which could be directly observable if flavour tagging were available.

A more conventional method to study the differences is to look at angular distributions among the four-jets. Several angles have been defined [45] to gauge the expected differences. As one example, in the production of $q\bar{q}g^*$, the g^* is polarized in the plane of the three-jet event, and this is reflected in its subsequent splitting: in $g^* \to gg$ the azimuthal angle distribution of g around the g^* direction slightly favours splittings in the event plane, while splittings out of the event plane are rather strongly favoured for $g^* \to q'\bar{q}'$. In ordinary QCD the latter process is infrequent, so the net result is close to zero. In the Abelian model the $g^* \to gg$ branchings are absent, while the $g^* \to q'\bar{q}'$ ones are strongly enhanced; thus out-of-the-event-plane splittings are strongly favoured. One trivial consequence is that, while the $q\bar{q}q'\bar{q}'$ fraction of four-jets is around 30% in the Abelian model with a y cutoff, it is more like 50% if instead a cutoff is used based on the aplanarity of events. (In some of the past literature, these two numbers have been mixed up, leading to unnecessary confusion and, at times, to an incorrect simulation of the Abelian model.)

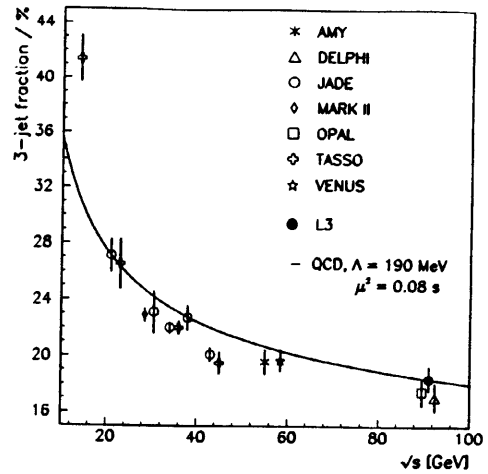

Figure 7: The three-jet fraction as a function of CM energy [21]. The three-jet definition is in terms of the JADE cluster algorithm [19], which is supposed to be insensitive to fragmentation effects (at least for CM energies above 20 GeV). Therefore a fixed α_S should have lead to a constant three-jet fraction, while the observed decrease with CM energy is in good agreement with QCD expectations.

Results have been presented from OPAL [46] and L3 [47], which both show that the Abelian model is excluded by current LEP data, based on the angular distributions in four-jet events, Fig. 6. However, the most interesting study is that of DELPHI [48], which attempts a two-dimensional analysis in two different angles at the same time, and which uses this to determine the ratio of Casimir operators N_C/C_F and T_R/C_F. This method thus can be used to check on the validity of QCD without any specific assumptions about alternative models — of course, as a by-product, again the Abelian model is excluded. Similar studies have also been made at TRISTAN [49], unfortunately with too low statistics to be as conclusive.

An independent indication for the validity of QCD comes from the running of α_S, Fig. 7, which is based on a study of the variation of the three-jet rates within some fixed y cuts, using the JADE clustering algorithm. The observed running agrees very well with QCD predictions. Thus, several of the fundamental properties of perturbative QCD have been tested at LEP, with good results.

3 Fragmentation

The fragmentation process has yet to be understood from first principles, starting from the QCD Lagrangian. This has left the way clear for the development of a number of different phenomenological models. Being models, none of them can lay claims to being 'correct'. The best one can aim for is a good representation of existing data, plus a predictive power for properties not yet studied or results at higher energies.

All existing models are of a probabilistic and iterative nature. This means that the fragmentation process as a whole is described in terms of one (or a few) simple underlying branchings, of the type jet $\to$ hadron + remainder-jet, string $\to$ hadron + remainder-string, cluster $\to$ hadron + hadron, or cluster $\to$ cluster + cluster. At each branching, probabilistic rules are given for the production of new flavours, and for the

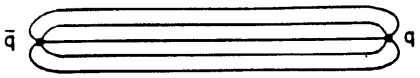

Figure 8: A uniform colour flux tube stretched between a q and a $\overline{q}$ endpoint — one possibility of visualizing the linear confinement property.

sharing of energy and momentum between the products.

Three main schools are usually distinguished, string fragmentation (SF), independent fragmentation (IF) and cluster fragmentation (CF) [50]. These need not be mutually exclusive; it is possible to have models which contain both cluster and string aspects, or models which interpolate between independent and string fragmentation.

While the evolution of fragmentation models was rapid in the early eighties, no really new algorithms have been introduced in the last five years, and only a modest amount of refinement of the existing approaches has been performed. New concepts, like local parton-hadron duality, and new experimental features, like intermittency, have recently led to a resurgence of fragmentation studies outside the framework of the existing programs. While very interesting, these studies have not yet led to fully-fledged programs of the kind needed to describe LEP events in full, and maybe they never will. A few examples of new ideas will appear later in this report, as a reminder for users to keep an open mind, given that nobody knows the ultimate truth.

3.1 String Fragmentation

The first example of a string fragmentation (SF) scheme was given by Artru and Mennessier [51]. With the elaborate string model developed by the Lund group in the years around 1980 [52], SF became more or less synonymous with the Lund model. However, also other SF or SF-inspired models exist.

3.1.1 The string concept

While nonperturbative QCD is not solved, lattice QCD studies lend support to a linear confinement picture (in the absence of dynamical quarks), i.e. the energy stored in the colour dipole field between a charge and anticharge increases linearly with the separation between the charges, if the short-distance Coulomb term is neglected. This is quite different from the behaviour in QED, and is related to the presence of a three-gluon vertex in QCD. The details are not yet well understood, however.

The assumption of linear confinement provides the starting point for the string model, most easily illustrated for the production of a back-to-back $q\overline{q}$ jet pair. As the partons move apart, the physical picture is that of a colour flux tube (or maybe colour vortex line) being stretched between the q and the $\overline{q}$, Fig. 8. The transverse dimensions of the tube are of typical hadronic sizes, roughly 1 fm. If the tube is assumed to be uniform along its length, this automatically leads to a confinement picture with a linearly rising potential. In order to obtain a Lorentz covariant and causal description of the energy flow due to this linear confinement, the most straightforward way is to use the dynamics of the massless relativistic string with no transverse degrees of freedom [53]. The mathematical, one-dimensional string can be thought of as parametrizing the position of the axis of a cylindrically symmetric flux tube. From hadron spectroscopy the string constant, i.e. the amount of energy per unit length, is deduced to be $\kappa \approx 1$ GeV/fm. The expression 'massless' relativistic string is somewhat of a misnomer: κ effectively corresponds to a 'mass density' along the string.

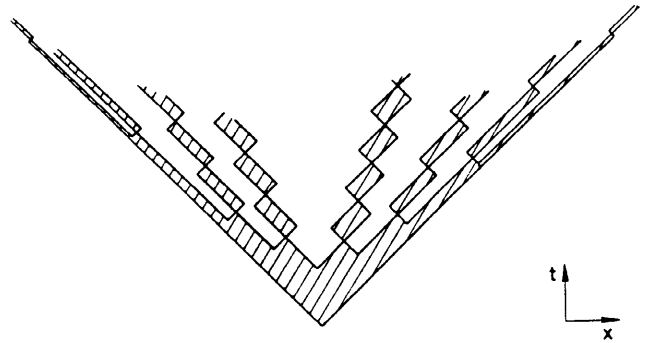

Figure 9: Breaking of a string in the Lund approach, into particles with discrete masses. Time is running upwards, and the longitudinal space dimension is horizontal. Massless quarks are moving along the light cone, corresponding to diagonal lines in the diagram. Hatched areas indicate regions of nonvanishing colour field. The quark from one break combines with the antiquark from the adjacent one to form a meson, in this figure represented by a sequence of rectangles (traced out by the 'yo-yo' motion of the quark and antiquark endpoints).

3.1.2 Fragmentation of a simple string

Let us now turn to the fragmentation process, and for simplicity consider a $q\overline{q}$ two-jet event. As the q and $\overline{q}$ move apart, the potential energy stored in the string increases, and the string may break by the production of a new $q'\overline{q}'$ pair, so that the system splits into two colour singlet systems $q\overline{q}'$ and $q'\overline{q}$. If the invariant mass of either of these string pieces is large enough, further breaks may occur. In the Lund string model, the string break-up process is assumed to proceed until only on-mass-shell hadrons remain, each hadron corresponding to a small piece of string, Fig. 9. Alternatively, string breaking may be stopped at a typical mass scale of one or a few GeV, where the string pieces are associated with clusters (see section 3.3).

In order to generate the quark-antiquark pairs $q'\overline{q}'$ which lead to string break-ups, the Lund model invokes the idea of quantum mechanical tunnelling. In terms of the transverse mass m_T of the q', the tunnelling probability (i.e. the probability that the $q'\overline{q}'$ will appear) is given by

$$\exp\left(-\frac{\pi m_T^2}{\kappa}\right) = \exp\left(-\frac{\pi m^2}{\kappa}\right)\exp\left(-\frac{\pi p_T^2}{\kappa}\right). \tag{22}$$

The factorization of the transverse momentum and the mass terms leads to a flavour-independent Gaussian spectrum for the p_T of $q'\overline{q}'$ pairs. Since the string is assumed to have no transverse excitations, this p_T is locally compensated between the quark and the antiquark of the pair. The total p_T of a hadron is made up out of the p_T contributions from the quark and antiquark that together form the hadron. In a perturbative QCD framework, a hard scattering is associated with gluon radiation, and further contributions to what is naively called fragmentation p_T comes from unresolved radiation. This is used as an explanation why the experimental $\langle p_T \rangle$ is somewhat higher than obtained with the formula above.

The formula also implies a suppression of heavy quark production $u : d : s : c \approx 1 : 1 : 0.3 : 10^{-11}$. Charm and heavier quarks hence are not expected to be produced in the soft fragmentation. Since the predicted flavour suppressions are in terms of quark masses, which are notoriously difficult to assign (should it be current algebra,

or constituent, or maybe something in between?), the suppression of $s\bar{s}$ production is left as a free parameter in the Lund program. At least qualitatively, the experimental value agrees with theoretical prejudice.

When the quark and antiquark from two adjacent string breakings are combined to form a meson, it is necessary to invoke an algorithm to choose between the different possibilities allowed, notably to choose between pseudoscalar and vector mesons. Here the string model is not particularly predictive. Qualitatively one expects a 1 : 3 ratio, from counting the number of spin states, multiplied by some wave function normalization factor, which should disfavour heavier states. Again, the relative composition is left as a free parameter in Monte Carlo implementations.

A tunnelling mechanism can also be used to explain the production of baryons. This is still a poorly understood area. In the simpest possible approach, a diquark in a colour antitriplet state is just treated like an ordinary antiquark, such that a string can break either by quark-antiquark or antidiquark-diquark pair production. The production probabilities are then given by the effective diquark masses assumed, plus simple flavour Clebsch-Gordan coefficients of the baryon wavefunctions. In this approach, the baryon and antibaryon are produced next to each other, and share (at least) two quark flavours. A more complex scenario is the 'popcorn' one, where diquarks as such do not exist, but rather quark-antiquark pairs are produced one after the other. Part of the time, this scenario gives back an effective diquark picture, but in addition configurations are possible where one or more mesons are produced in between the baryon and antibaryon, and where therefore these two are no longer required to be as strongly correlated in flavour content.

In general, the different string breaks are causally disconnected, see Fig. 9. This means that it is possible to describe the breaks in any convenient order, e.g. from the quark end inwards. One therefore is led to write down an iterative scheme for the fragmentation, as follows. Assume an initial quark q moving out along the $+z$ axis, with the antiquark going out in the opposite direction, and with total light cone momentum $W_+ = E + p_L$, where $p_L = p_z$ is the longitudinal momentum along the jet axis. By the production of a $q_1\bar{q}_1$ pair, a meson $q\bar{q}_1$ is produced, leaving behind an unpaired quark q_1. The sharing of the W_+ is given by some probability distribution $f(z_1)$, where z_1 is the fraction taken by the hadron, with $1 - z_1$ left for the remainder-jet q_1. A second pair $q_2\bar{q}_2$ may now be produced, to give a new meson $q_1\bar{q}_2$, which takes a fraction z_2 of the remaining light cone energy and momentum, $(1 - z_1)W_+$, etc. This process may be iterated until all energy is used up, with some modifications close to the $\bar{q}$ end of the string to make total energy and momentum come out right. By the relation $(E + p_L)(E - p_L) = m_T^2 = m^2 + p_T^2$, the peeling off of W_+ in fact also implies a reduction in the available $W_- = E - p_L$; it is necessary to conserve both.

The choice of starting the fragmentation from the quark end is arbitrary, however. A fragmentation process described in terms of starting at the $\bar{q}$ end of the system and fragmenting towards the q end should be equivalent. This 'left-right' symmetry constrains the allowed shape of fragmentation functions $f(z)$, where z is once again the fraction of $E + p_L$ along the jet axis chosen, i.e. $p_L = \pm p_z$ for quark/antiquark. Under some simplifying assumptions, the left-right symmetric fragmentation function takes the form

$$f(z) \propto \frac{1}{z}(1 - z)^a \exp(-bm_T^2/z), \tag{23}$$

with the two free parameters a and b.

If the objects produced during string break-up are not on-shell hadrons, as is the case e.g. in the Artru-Mennessier model, the logical recipe is to have a constant probability for the string to break per unit of invariant space-time area swept out by the string. This gives an exponential area decay law, if one remembers that a string can not break in the forwards light cone of an earlier break, i.e. when it has 'already' broken. Further, left-right symmetry is ensured. The specification of adjacent break-

ups in the two-dimensional sheet of the string can be translated into a simultaneous probability distribution in the mass-squared and the z of the produced cluster:

$$\frac{d\mathcal{P}}{dm^2dz} \propto \frac{1}{z}\exp(-bm^2/z), \tag{24}$$

with b a free parameter proportional to the probability of break-up per invariant unit of string area. The mass-spectrum can be obtained by integrating out z, and is proportional to $\mathrm{E}_1(bm^2)$, i.e. it possesses a logarithmic divergence at small masses (in programs often removed by a minimum cluster mass requirement). Once the m^2 is given, the fragmentation function can be read off eq. (24), i.e. it is exactly the same as was obtained in the discrete mass case, eq. (23), except that $a = 0$. The similarity in the final result is all the more surprising, since a discrete mass spectrum implies that string breaks are allowed only along one-dimensional hyperbolae, rather than inside two-dimensional areas.

3.1.3 Fragmentation of a multiparton system

If several partons are moving apart from a common origin, the details of the string drawing become more complicated. For a $q\bar{q}g$ event, a string is stretched from the q end via the g to the $\bar{q}$ end, i.e. the gluon is a kink on the string, carrying energy and momentum, Fig. 10a. As a consequence, the gluon has two string pieces attached, and the ratio of gluon/quark string force is two, a number which can be compared with the ratio of colour charge Casimir operators, $N_C/C_F = 2/(1 - 1/N_C^2) = 9/4$. In this, as in other respects, the string model can be viewed as a variant of QCD where the number of colours N_C is not 3 but infinite. Note that the factor 2 above does not depend on the kinematical configuration: a smaller opening angle between two partons corresponds to a smaller string length drawn out per unit time, but also to an increased transverse velocity of the string piece, which gives an exactly compensating boost factor in the energy density per unit string length.

Consider the string motion in a $q\bar{q}g$ event. In the string piece between the g and the q ($\bar{q}$), g four-momentum is flowing towards the q ($\bar{q}$) end and q ($\bar{q}$) four-momentum towards the g end. Such packets of energy and momentum are called 'genes' [53]. When the gluon has lost all its energy, the g four-momentum continues moving away from the middle (i.e. where the gluon used to be), and instead a third string region is formed there, consisting of inflowing q and $\bar{q}$ four-momentum, Fig. 10a. If this third region would only appear at a time later than the typical time scale for fragmentation, it could not affect the sharing of energy between different particles. This is true in the limit of high energy, well separated partons.

For a small gluon energy, on the other hand, the third string region appears early, and the overall drawing of the string becomes fairly two-jetlike, Fig. 10b. In the limit of vanishing gluon energy, the two initial string regions collapse to naught, and the ordinary two-jet event is recovered. Also for a collinear gluon, i.e. θ_{qg} (or $\theta_{\bar{q}g}$) small, the stretching becomes two-jetlike, Fig. 10c. These properties of the string motion are the reason why the string fragmentation scheme is 'infrared safe' with respect to soft or collinear gluon emission.

In an event with several gluons, these still will appear as kinks on the string between the q and $\bar{q}$ ends. With several gluons present, the full string evolution may become rather complicated, but the basic principles remain the same as outlined for three-jet events. In particular two nearby partons (with matching colours) always collectively draw out the string.

For four-jet events (or events with more than four jets) which are generated using matrix elements, there are several possible topologies for the ordering of partons along the string. This is illustrated in Fig. 11 for $q\bar{q}gg$ events. A knowledge of quark and gluon colours, obtained by perturbation theory, would uniquely specify the stretching

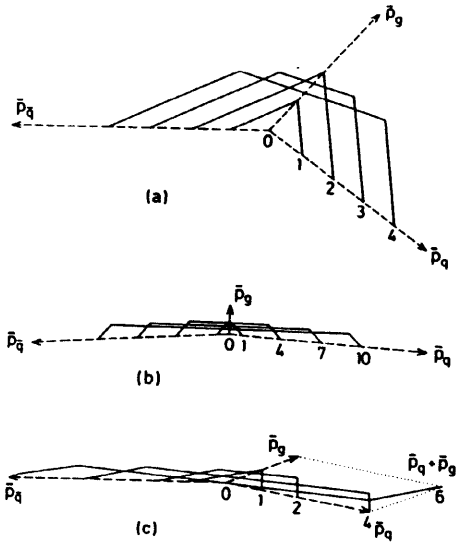

Figure 10: The string drawing for (a) an ordinary three-jet event, (b) a three-jet event with a soft gluon, and (c) a three-jet event with a collinear gluon. Dashed lines give the momenta (and hence the trajectories) of the partons. Full lines give the string shape at different times, with numbers representing time in some suitable scale.

of the string [54], so long as the two gluons do not have the same colour. The probability for the latter is down in magnitude by a factor $1/N_C^2$, where $N_C = 3$ is the number of colours. Perturbative QCD gives no answer on how to handle these situations, but recipes have to be included in event generators.

In leading log shower programs, where only $1 \to 2$ branchings are included, the rules for colour flow in branchings are well-defined.

- $q \to qg$: the original colour of the quark is taken by the gluon, and a new colour-anticolour pair is shared by quark and gluon.
- $g \to gg$: the original colour is inherited by one gluon and the anticolour by the other, again a new colour-anticolour pair is shared.
- $g \to q\bar{q}$: the original colour goes to the quark and the anticolour to the antiquark; this means that the original string going through the gluon is split into two.

If one goes beyond this approximation, as in NLLjet, the same problems will arise as in the four-jet matrix elements, and similar solutions have to be found.

Whichever scenario is considered, matrix elements or showers, there is a tacit

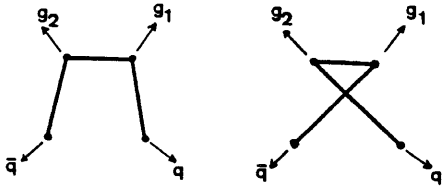

Figure 11: The two different ways of stretching a string in a $q\bar{q}gg$ event.

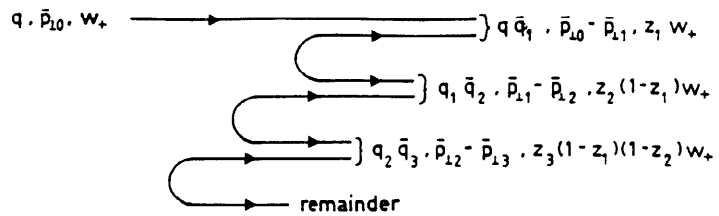

Figure 12: The iterative ansatz for flavour, transverse momentum, and light-cone energy-momentum ($W_+ = E + p_L$) fraction.

assumption that soft gluon exchanges between partons will not mess up the original colour assignment. Both theoretical and experimental arguments can be raised as to why this might be a fair approximation, but eventually this assumption is something which needs more rigorous testing [55].

3.2 Independent Fragmentation

The independent fragmentation (IF) approach dates back to the early seventies [56], and gained widespread popularity with the Field-Feynman paper [57]. Subsequently, IF was the basis for two programs widely used in the early PETRA/PEP days, the Hoyer *et al.* [58] and the Ali *et al.* [59] programs. These programs have not been updated since their conception, and therefore are not well suited for LEP physics studies. Anyway, as will be seen, the IF concept very much is in disrepute these days, and what little use there is can be fully covered by the IF options available in JETSET.

In the IF approach, it is assumed that the fragmentation of any system of partons can be described as an incoherent sum of independent fragmentation procedures for each parton separately. The process is to be carried out in the overall CM frame of the jet system, with each jet fragmentation axis given by the direction of motion of the corresponding parton in that frame.

3.2.1 Single jet fragmentation

As in the case of SF, the fragmentation of a jet is described iteratively, see Fig. 12. From an original quark jet q, hadrons are split off one by one, leaving behind new remainder-jets with scaled-down energies. The function $f(z)$, which describes how big a fraction z of the remaining energy is taken by the hadron, is assumed to be the same at each step, i.e. independent of remaining energy. No special philosophy constrains the choice of $f(z)$, so several different proposals exist in the literature. If z is interpreted as the fraction of the jet $E + p_L$, this leads to a flat central rapidity plateau dn/dy for a large initial energy.

The normal z interpretation means that a choice of a z value close to 0 corresponds to a particle moving backwards, i.e. with $p_L < 0$. It makes sense to allow only the production of particles with $p_L > 0$, but to explicitly constrain z accordingly would destroy longitudinal invariance. The most straightforward way out is to allow all z values but discard hadrons with $p_L < 0$. Flavour, transverse momentum and $E + p_L$ carried by these hadrons are 'lost' for the forward jet. The average energy of the final jet comes out roughly right this way, with a spread of 1 - 2 GeV around the mean. The jet longitudinal momentum is decreased, however, since the jet acquires an effective mass during the fragmentation procedure. For a two-jet event this is as it should be, at least on average, because also the momentum of the compensating opposite-side parton is decreased.

Each splitting corresponds to the production of a $q'\overline{q}'$ pair. The relative composition of these pairs is parametrized as in the string model, with corresponding possibilities to extend the model also to baryon production. Also the way in which the q_1 from one break is combined with the $\overline{q}_2$ from an adjacent break to form the different possible hadrons is the same, as is the way the transverse momenta from the constituent quarks are added to give the transverse momentum of the hadron. The main differerence, at this point, is that the string model is based on a specific underlying space-time picture of the fragmentation process, while the iterative approach is introduced *ad hoc* in independent fragmentation.

Contrary to the string model, however, within the IF framework there is no unique recipe for how gluon jet fragmentation should be handled. One possibility is to treat it exactly like a quark jet, with the initial quark flavour chosen at random among $u, \overline{u}, d, \overline{d}, s$ and $\overline{s}$, including the ordinary s quark suppression factor. Since the gluon is supposed to fragment more softly than a quark jet, the fragmentation function may be chosen independently. Another common option is to split the g jet into a pair of parallel q and $\overline{q}$ ones, sharing the energy, e.g. according to the Altarelli-Parisi splitting function in eq. (18). The fragmentation function could still be chosen independently, if so desired. Further, in either case the fragmentation p_T could be chosen to have a different mean.

3.2.2 Fragmentation of a jet system

The concept of IF inevitably leads to the total flavour, energy and momentum not being exactly conserved in the fragmentation process proper. At the end of the generation, special algorithms are therefore used to patch this up.

Usually little attention is given to flavour conservation. Typically, that aspect is solved by reassigning the flavour content of centrally produced particles, without changing their three-momenta, in such a way that the net number of each flavour is vanishing.

Several different schemes for energy and momentum conservation have been devised. One [58] is to conserve transverse momentum locally within each jet, so that the final momentum vector of a jet is always parallel with that of the corresponding parton. Then longitudinal momenta may be rescaled separately for particles within each jet, such that the ratio of rescaled jet momentum to initial parton momentum is the same in all jets. Since the initial partons had net vanishing three-momentum, so do now the hadrons. The rescaling factors may be chosen such that also energy comes out right. In another common approach [59] a generated event is boosted to the frame where the total hadronic momentum is vanishing. After that, energy conservation can be obtained by rescaling all particle three-momenta by a common factor.

Depending on what choice is made, the implementation of momentum conservation may either force three-jet events to become even more three-jetlike, or to become more two-jetlike. As a consequence, the α_S value needed to describe data can be rather different. The difference decreases with increasing CM energy, but could still be 20% – 30% at LEP energies. The discarding of independent fragmentation models is the main reason why the range of published α_S values is so much smaller at LEP energies than it was at PETRA, not the higher energies or the refined choice of observables.

A serious conceptual weakness of the IF framework is the issue of Lorentz invariance. The outcome of the fragmentation procedure depends on the coordinate frame chosen, a problem circumvented by requiring fragmentation always to be carried out in the CM frame. This is a consistent procedure for two-jet events, but only a technical trick for multijets.

It should be noted, however, that a Lorentz covariant generalization of the independent fragmentation model exists, in which separate 'gluon-type' and 'quark-type'

strings are used, the Montvay scheme [60]. For a three-jet event, the three string pieces are joined at a junction. The motion of this junction is determined by the vector sum of the string tensions acting on it. In particular, it is always possible to boost an event to a frame where this junction is at rest. In this frame, much of the standard naive IF picture holds for the fragmentation of the three jets; additionally, a correct treatment would automatically give flavour, energy and momentum conservation. Unfortunately, while the scheme is perfectly valid also with several gluon jets present, it is then very complicated to write an event generator based on it, and nobody has ever done so.

Another weakness of IF is the issue of collinear divergences. In a parton shower picture, where a quark or gluon is expected to branch into several reasonably collimated partons, the independent fragmentation of one single parton or of a bunch of collinear ones gives quite different outcomes, e.g. with a much larger hadron multiplicity in the latter case. Results therefore are sensitive to the choice of shower cutoff scale Q_0: any working set of fragmentation functions would have to be retuned significantly if Q_0 were changed.

As we will see in section 4.5, actually IF fails to describe the 'string effect'. This means that also from an experimental point of view, IF is not a particularly interesting model anymore. Attempts are occasionally made to revive IF [61], but these are not particularly convincing.

3.3 Cluster Fragmentation

While the Artru-Mennessier model [51] contained clusters, dedicated cluster models were first developed at CALTECH [62]. Today, cluster models are found in HERWIG and in the CALTECH-II program [63]. The main difference between existing cluster fragmentation (CF) schemes is the extent to which string fragmentation ideas are incorporated.

- In one extreme, a parton shower picture is used to produce a partonic configuration. At the end of the shower evolution, remaining gluons are split forcibly into $q\overline{q}$ pairs. With colour explicitly kept track of, the quark of one splitting may be combined with the antiquark from an adjacent one to form a colourless cluster, Fig. 13. These clusters subsequently decay into the final hadrons. This is, more or less, the HERWIG strategy.
- In the other extreme, parton showers or matrix elements may be used to generate a partonic configuration, with strings stretched in between the partons, as described in the SF section. These strings then fragment into clusters, which again decay into the final hadrons. Fig. 14 illustrates this approach, which is found in CALTECH-II.

3.3.1 The cluster concept

The concept of cluster fragmentation offers the great promise of a simple, local and universal description of hadronization. Gone are the long, ordered fragmentation chains present both in SF and IF. In their place appear simple clusters, which are assumed to be the basic units from which the hadrons are produced. A cluster is ideally only characterized by its total mass and total flavour content, i.e. unlike a string it does not possess an internal structure. If the shower evolution and/or string breaks are chosen such that most clusters have a mass of a few GeV, the cluster mass spectrum may be thought of as a superposition of fairly broad (i.e. short-lived) resonances. Phase-space aspects may then be expected to dominate the decay properties. This applies both for the selection of decay channels, and for the kinematics of the decay. Thus a decay is assumed to be isotropic in the rest frame of the cluster. This gives a compact description with few parameters. In particular, the separate longitudinal and transverse momentum fragmentation descriptions in SF and IF are here replaced

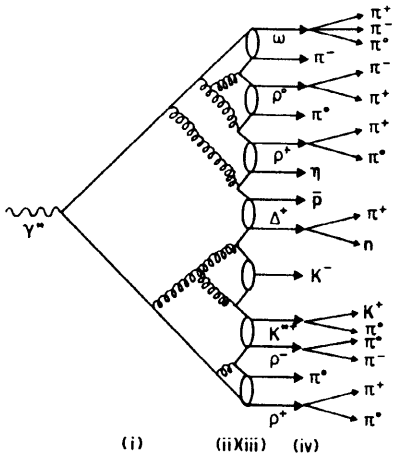

Figure 13: One cluster fragmentation scenario: (i) shower evolution, (ii) forced $g \to q\bar{q}$ branchings, (iii) cluster formation, and (iv) cluster decay. Occasionally, a cluster is associated with a single particle.

by a unified framework, wherein parton showers and cluster phase-space decays give the full momentum distribution. As we shall see in the following paragraphs, there are some complications, however.

Ideally, parton shower evolution should in itself give a cluster mass spectrum strongly damped at masses above a few GeV, so that two-body decays of clusters would give a sufficient description. This was the hope in the early days of CF, a hope founded on the concept of 'preconfinement' [64]. Unfortunately, despite the preconfinement property, there is no known way of avoiding a rather large spread of cluster

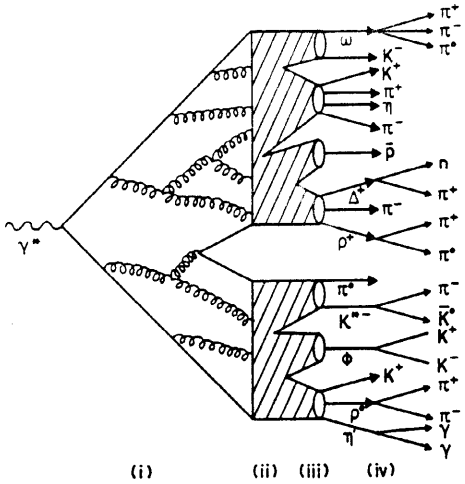

Figure 14: Another cluster fragmentation scenario: (i) shower evolution, (ii) string evolution and break-up into (iii) clusters, (iv) cluster decay into a varying number of particles.

masses. In programs, it is therefore necessary to introduce the possibility for a high-mass cluster to produce more than two hadrons. This is typically done by allowing branchings cluster $\to$ cluster + hadron or cluster $\to$ cluster + cluster.

3.3.2 Cluster formation and decay

Flavours are generated at several different stages. First, at the branchings $g \to q\bar{q}$, alternatively at the string breaks, i.e. when the clusters are formed. In CALTECH-II the relative probabilities appear as explicit parameters, while they are given by the parton mass assignments in HERWIG. In the original Webber-Marchesini model, only quark-antiquark pairs (or gluons) were created at branchings. This leads to some problems in the description of baryon production, see section 4.3.4. The present model therefore also includes, as an option, the possibility that a gluon may branch into a diquark-antidiquark pair. This process is turned on below some scale in the shower evolution, with an arbitrary strength relative to ordinary $q\bar{q}$ production.

A second stage of flavour production occurs when larger clusters decay into smaller ones. Typically, this means that a cluster $q_1\bar{q}_2$ breaks, by the production of an intermediate $q_3\bar{q}_3$ pair, into clusters $q_1\bar{q}_3$ and $q_3\bar{q}_2$. One of the two may, but need not, be directly associated with a hadron. In general, the symbol q may here represent either a quark or an antidiquark.

The third stage of flavour production is when a cluster decays into two hadrons. The flavour flow is as above, i.e. a new $q_3\bar{q}_3$ pair splits the old cluster in the middle. Again quark and diquark production is allowed, with relative probability dictated by phase-space alone.

The phase-space assumption means that each allowed cluster decay channel is assigned a weight proportional to the density of states, $(2s_1+1)(2s_2+1)(2p^*/m)$. Here s_1 and s_2 are the spins of the two hadrons produced, and p^* the common momentum of the products in the rest frame of the decaying cluster (with mass m). The weight gives the relative probability of the choice being retained; in case of rejection a new q_3 flavour is selected and the procedure repeated.

It should be noted that the new q_3 quark flavour is not associated with any dynamical properties, such as a mass or, for diquarks, a total spin. It is only the properties of the final, 'observable' particles that can influence the relative production rate. Further, the 'fragmentation' transverse momentum is determined by the average energy release in cluster decay, and in subsequent resonance decays, as opposed to the extra parameter needed in SF or IF.

In the decay of a large cluster into two, the kinematics is usually handled anisotropically, along the 'string' direction. The same kind of phase-space weight may still be used, provided clusters are assigned suitable spins and a cluster mass spectrum weight is folded in.

If all clusters are to decay into at least two particles, the probability of producing a single particle carrying a large fraction of the total jet energy is severely underestimated. Therefore cluster programs usually contain a mechanism, so that a sufficiently light cluster is assumed to collapse into a single particle. Four-momentum is shuffled to or from nearby clusters, so as to achieve overall energy and momentum conservation.

3.4 Other Fragmentation Approaches

As should be amply clear from the discussions above, the study of fragmentation is not a closed chapter, with one simple framework that does it all. In addition, none of the models discussed are able to describe all experimental features. This means that a broad spectrum of alternatives should be pursued. A few alternatives are described in [3]. They include the following ones.

- Local Parton-Hadron Duality (LPHD) [26]. In this approach, the fragmentation step is done away with altogether: by continuing the parton shower approach down to very small virtualities, a situation is reached where partons can be identified on a one-to-one basis with the final observable hadrons. How flavours and flavour correlations should be introduced in this approach is not addressed, but all kinds of energy and multiplicity correlations can be predicted analytically, and successfully.
- Intermittency models. Given the large interest in intermittency, a number of toy models have been developed to describe non-Poissonian particle production processes, which would give rise to additional fluctuations compared to the standard fragmentation approaches [65].
- Topological models. In a model proposed by Ellis and Kowalski, baryons are produced at topological defects [66]. These defects appear when chiral symmetry is broken during the fragmentation phase, and adjacent domains (corresponding to the final mesons) have a mismatch in chiral direction. A main prediction is a larger rate of baryon production at LEP energies than in conventional models.
- Non-QCD models. It may be interesting to see whether it is possible to construct models which do not make any explicit reference to standard QCD, and yet can be made to describe data. A few different suggestions are here available, where the original fragmenting object is an excited hadron with the full CM energy of the event, which cascades over a sequence of other excited hadron states down into the final light hadrons [67]. In this kind of approach, there is no reference at all to a quark/gluon phase at early times of the fragmentation.

3.5 Particles and Their Decays

A large fraction of the particles produced by fragmentation are actually unstable, and subsequently decay into the observable stable (or almost stable) ones. It is therefore important to include all particles with their proper mass distributions and decay properties. In fact, although involving little of deep physics, this is less trivial than it may sound: much information is available in the Review of Particle Properties [16], but there is also very much missing. If one goes beyond the lowest-lying pseudoscalar or vector meson multiplets, then many multiplet members are poorly known. One still gets by, since the contribution from higher multiplets usually is assumed to be small, or at least to give small effects in the observable hadron distributions.

Many resonances are very short-lived, so that a simple Breit-Wigner description of the mass distribution is not realistic. However, to include the correct shape is messy, since then the production and the decay of a particle become intertwined. Therefore usually simplified approaches are introduced, which work fine for general event shapes, but are insufficient for detailed studies of resonance production.

Further, the decay treatment involves a guessing at branching ratios when these are poorly known, like for B mesons. Even when a large fraction of the decays are known, like for the D mesons, the decay channels used in a program have to add up to 100%, i.e. extra plausible decay channels have to be added by hand. Also with the decay products known, it is often not sufficient just to distribute them according to phase space. An obvious example is weak semileptonic decays, where the produced electron or muon is well measured experimentally, and an accurate modelling is required e.g. to separate contributions from b and c quarks for quark tagging.

Finally, the effects of particle polarization often are neglected: particles are assumed to decay isotropically. In τ decays we know this is not correct, and there are also other cases where polarization effects might be important.

4 Experimental Knowledge

There are several reviews of results in e^+e^- physics at lower energies [68,50], and a summary of LEP QCD results is found in [25]. In this section therefore the objective is to illuminate the interplay between model building and experimental tests. For this purpose, a few examples will be picked.

4.1 Event Characterization Methods

Since the typical LEP hadronic event contains 20 charged particles and as many neutral ones, it is convenient to characterize an event in terms of collective variables. These variables may be classified as event measures, cluster topologies, one-particle inclusive distributions, two-particle inclusive correlations, etc.

The list of one-particle inclusive distributions include transverse and longitudinal momentum spectra, rapidity distributions, etc. The most well-known two-particle inclusive distribution is probably the energy-energy correlation [69]

$$EEC(\theta) = \sum_{i<j} \frac{2E_iE_j}{E_{CM}^2}\delta(\theta - \theta_{ij}), \tag{25}$$

and its asymmetry $EECA(\theta) = EEC(\pi - \theta) - EEC(\theta)$.

4.1.1 Thrust and Sphericity

One frequently used family of event measures is the thrust one [70]. Thrust T is defined as

$$T = \max_{|\overline{n}|=1} \frac{\sum_i |\overline{p}_i\overline{n}|}{\sum_i |\overline{p}_i|}, \tag{26}$$

where the index i runs over all the particles of the event, and where the axis $\overline{n}$ for which maximum is obtained is called the thrust axis. Ideal two-jet events have $T = 1$, while perfectly spherical events have $T = 1/2$. Major is defined the same was as thrust, but with the major axis constrained to be orthogonal to the thrust one. The minor axis is chosen orthogonal both to the thrust and to the major ones, and the minor measure is defined as the scaled sum of projected momenta along this axis, just like for thrust and major. The difference between major and minor is called oblateness.

Another frequently used family is the sphericity one [71]. Here one defines a tensor

$$S^{ab} = \frac{\sum_i p_i^a p_i^b}{\sum_i p_i^2}, \tag{27}$$

with $a, b = 1, 2, 3$ corresponding to the x, y and z directions in space. From the three eigenvalues $\lambda_1 > \lambda_2 > \lambda_3$, with sum unity, one may construct sphericity $S = 3(\lambda_2 + \lambda_3)/2$ and aplanarity $A = 3\lambda_3/2$. The former quantity runs between 0 and 1, with 0 corresponding to ideal two-jets and 1 to spherical events. The eigenvectors of the tensor can be used to define an event axis and an event plane.

Both the thrust and the sphericity family have their advantages and disadvantages [72]. There is no simple fast recipe to find the correct thrust axis; either one has to pick a slow algorithm or an approximate one. Further, the behaviour of the thrust axis can be pathological: a slight change of the momenta in an event can flip the axis to an altogether different position. The sphericity axis is easy to find, but the sphericity measure itself suffers from the disadvantage of being quadratic in momenta. This means that, if one single particle is split into two collinear ones, the sphericity measure and sphericity axis is changed, i.e. sphericity is sensitive to irrelevant details

of parton branchings and particle decays. Therefore the limiting procedure of eq. (4) does not work, i.e., unlike thrust, sphericity cannot be calculated perturbatively.

Considering these known facts, it is maybe surprising that so little attention has been given to using better, or at least alternative, methods, in particular since such are already known. The most obvious is to use a linearized version of the sphericity method, i.e. to replace the sphericity tensor above by [73]

$$S^{ab}_{lin} = \frac{\sum_i p^a_i p^b_i / |\overline{p}_i|}{\sum_i |\overline{p}_i|}, \tag{28}$$

i.e. where one power of $|\overline{p}_i|$ has been removed from both numerator and denominator. This measure can be diagonalized just like the sphericity one, and eigenvectors are easy to find. Yet it is linear in momentum, and therefore infrared safe and perturbatively calculable. What little experience we have also indicates that event axes found this way are every bit as good, however that should be defined, as either sphericity or thrust axes.

4.1.2 Cluster algorithms

The usage of cluster algorithms has become more and more widespread. Today, the JADE algorithm [19] is the most popular one. In this algorithm a distance measure between clusters i and j is defined by

$$y_{ij} = \frac{2E_iE_j(1-\cos\theta_{ij})}{E^2_{vis}}, \tag{29}$$

where E_{vis} is the total visible energy of the event. (The usage of E_{vis} in the denominator, rather than e.g. E_{CM}, tends to make the measure less sensitive to detector acceptance corrections.) The algorithm works as follows. Initially there is one cluster for each of the particles of the event. The y_{ij} value is calculated for each cluster pair, and the pair with the smallest y_{ij} is joined into one single cluster, with four-momentum given by adding the constituent four-momenta. The event now has one cluster less. Once again the pair with smallest y_{ij} is found, a new joining is made, etc. The recombination procedure is iterated until all distances $y_{ij} > y_{cut}$, where y_{cut} is a predetermined jet resolution power. The larger the y_{cut} scale, the smaller the final number of clusters.

The JADE algorithm has several advantages. The y_{cut} scale is very closely related to the y resolution parameter defined in the matrix element description (section 2.1.1). Specifically, if y_{cut} is chosen equal to y, the distribution in the number of clusters found very closely matches the generated parton distribution. This gives a direct possibility to test perturbative QCD with a minimum of worry about nonperturbative effects.

The successes of the JADE algorithm are legio. It is maybe therefore necessary to issue a general warning against blind faith in it.

- The algorithm is not Lorentz covariant, contrary to what is sometimes claimed. It is well known (since ten years or so) that an algorithm which uses the true invariant mass, i.e. $(E_i+E_j)^2 - (\overline{p}_i+\overline{p}_j)^2$ rather than $2E_iE_j(1-\cos\theta_{ij})$, is unstable: such an algorithm will start the clustering where most particles are to be found, i.e. in the center of the event, and give quite funny clustering assignments. The JADE algorithm breaks Lorentz covariance by favouring clustering of faster particles over that of central ones, and thus gives more reasonable results. Premature joinings of central particles still remains one of the major problems of the algorithm.
- The algorithm is not insensitive to fragmentation effects. It is true that, if string fragmentation is used, the number of clusters on the parton and on the hadron level agree well, at least for reasonably large CM energies. However, if independent fragmentation were to be used, quite large fragmentation corrections would appear. Thus, if the situation today looks much simpler than it did in the old PETRA/PEP days, it is not so much because we have hit on more fragmentation model independent measures, but rather because a number of fragmentation models taken seriously then are no longer in use today.
- While the JADE algorithm does a good job of finding the number of partons, it is not optimal for finding jet directions or energies. One reason is that the distance measure allows the joining of particles which go in quite different directions, if only they are soft. Another is that two particles, once joined, can never be reassigned to separate final clusters. Thus, in the angular region between two jets, a set of low-energy particles could be joined at an early stage, and then go *en masse* to one of the jets.

It may be interesting to compare with another cluster algorithm, such as the one found in JETSET [74]. Here the distance measure is

$$d_{ij} = \frac{2p^2_ip^2_j(1-\cos\theta_{ij})}{(p_i+p_j)^2}. \tag{30}$$

For two nearby particles ($\sin\theta_{ij} \approx 2\sin(\theta_{ij}/2)$) the d_{ij} measure has a simple geometrical interpretation as the p^2_T of each of the two particles with respect to their vector sum. The underlying physics idea is to define a jet as a collection of particles with a limited transverse momentum with respect to the jet direction, rather than as a collection of particles with a small invariant mass.

The algorithm works the same way as the JADE one, in that the number of clusters is successively reduced by one, until all cluster pairs are separated by a distance above some cutoff value. However, after each joining, all particles of the event are reassigned to the cluster to which they are closest, again in terms of the d_{ij} measure. If some low-momentum cluster is formed at an early stage, it can thus very well later be split between two high energy jets.

The net result of these two differences is that the JETSET algorithm gives narrower jets, which better agrees with the naive visual impression of jet structure than the JADE algorithm clusters do, and that jet directions are better reconstructed. For four-jet (triple gluon vertex) studies it is therefore likely to be the better algorithm. However, the number of clusters reconstructed agrees less well with the number of partons above some given y cut, the algorithm is even less Lorentz covariant than the JADE one, and it is every bit as much fragmentation model dependent. It is therefore not a panacea — today we do not have *one* algorithm that is best for everything!

4.2 Event Shapes

A number of event shape studies at LEP have already been presented [75]; two examples of the distributions obtained are given in Fig. 15. Generally, very good agreement is obtained between the data and models based on parton showers plus string or cluster fragmentation, be that JETSET, HERWIG or ARIADNE. It is not even necessary to tune the parameters of the programs to LEP data; already the values determined at around 30 GeV [76,77] give quite good descriptions.

A closer look reveals some interesting patterns. All programs provide a better description of LEP data than they do of PETRA/PEP data. Since the parton shower aspects are more dominant at larger energies, relative to fragmentation effects, this would indicate that the shower is fairly well simulated in all the programs studied. Despite large superficial differences, the JETSET, HERWIG and ARIADNE shower algorithms are pretty much based on the same kind of approach to the parton production process, and this approach indeed seems very successful — good news for

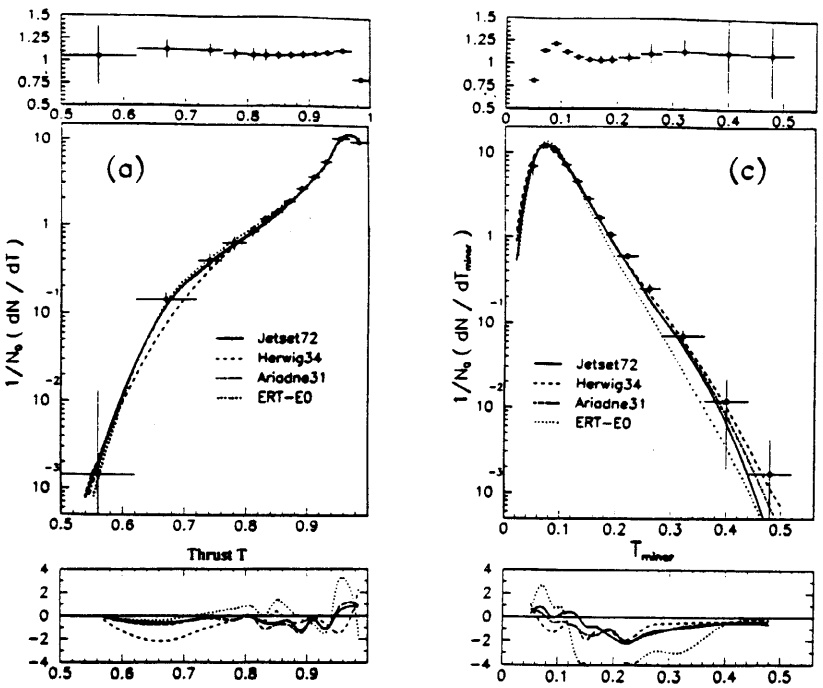

Figure 15: The thrust and minor distributions observed by OPAL, compared with the results of a few models [75]. Top: correction factors applied to the data for unfolding of detector effects. Bottom: difference between model predictions and data, in units of standard deviation.

experimentalists who need extrapolations to higher energies.

Conversely, the fact that agreement is worse at lower energies tends to indicate that fragmentation aspects are not as well modelled as are the parton shower ones. Here we also see a marked difference between JETSET and HERWIG, with the latter providing a clearly worse description at PETRA/PEP. In other words, most likely the cluster fragmentation model of HERWIG is inferior to the string one of JETSET.

Matrix element based models, if tuned at lower energies, fail miserably to describe LEP data. Particle multiplicities are too small and jets too narrow; one way or another this is reflected in distribution after distribution. These shortcomings can all be traced to the inability to account for multiple (semi)soft gluon emission, because of the need to keep sensical two-, three- and four-jet rates, i.e. to use cutoffs $y \geq 0.01$. The failure of the matrix element approach at LEP was predicted beforehand [76], and fits well in with our current picture of perturbative QCD, where parton showering is assumed to go on down to mass scales of around 1 GeV, much below acceptable matrix element cutoffs.

Granted that no energy-independent parametrization is possible in the matrix element approach, one may wonder if it is possible to tune parameters separately for each energy. In particular, could one make the fragmentation function softer and the fragmentation transverse momentum larger as the CM energy is increased, i.e. try to include the emission of soft gluons into some effective fragmentation parameters, in such a way that good agreement could still be obtained with LEP data? When this approach was tried years ago, at PETRA/PEP/TRISTAN energies, the answer

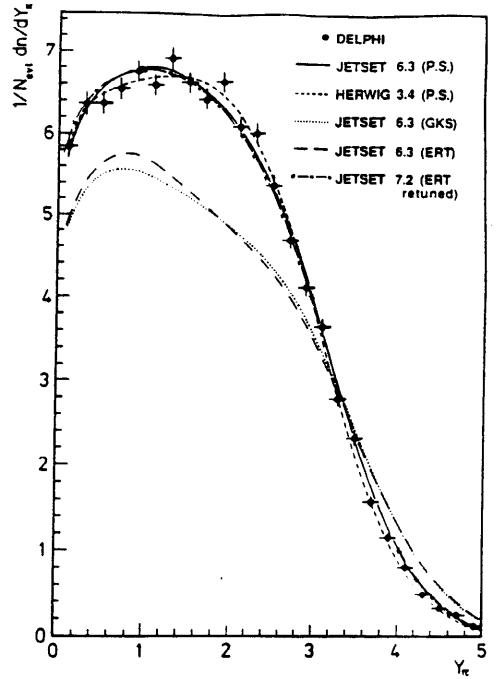

Figure 16: The rapidity distribution of charged particles (assumed to be all pions) with respect to the thrust axis, for shower programs (P.S.), matrix element programs extrapolated from lower energies (GKS and ERT), and for retuned matrix elements (ERT retuned), from DELPHI [75].

was no: already there the matrix element approach was clearly inferior to the parton shower one [76,77,78]. The outcome at LEP was therefore never in doubt.

However, a new aspect has entered the game in the last few years: optimized perturbation theory. Many of the problems of the past were related to the lack of four-jet events in the matrix element implementations. When today we allow ourselves the additional freedom of increasing the four-jet rate by the use of a lower Q^2 scale in α_S, in fact it is possible to achieve quite good agreement between data and matrix elements even at LEP energies [79], see e.g. Fig. 16. This is rather a disappointment, since it indicates that any attempt to look at jet structures beyond four-jets will have to cope with an overwhelming fragmentation background. One of the tasks of the future will be to find measures where the tuned-up matrix element approach fails, and from there to gain increased understanding of soft gluon emission.

4.3 Multiplicities and Correlations

4.3.1 Multiplicity distributions

The average charged multiplicity at LEP agrees well with QCD extrapolations from lower energies [75,80], both for analytical formulae and for parton shower based programs. However, as already noted, a matrix element approach with fixed fragmentation parameters gives too slow an increase of multiplicity with energy.

Also the multiplicity distribution itself is well described in models. If plotted in

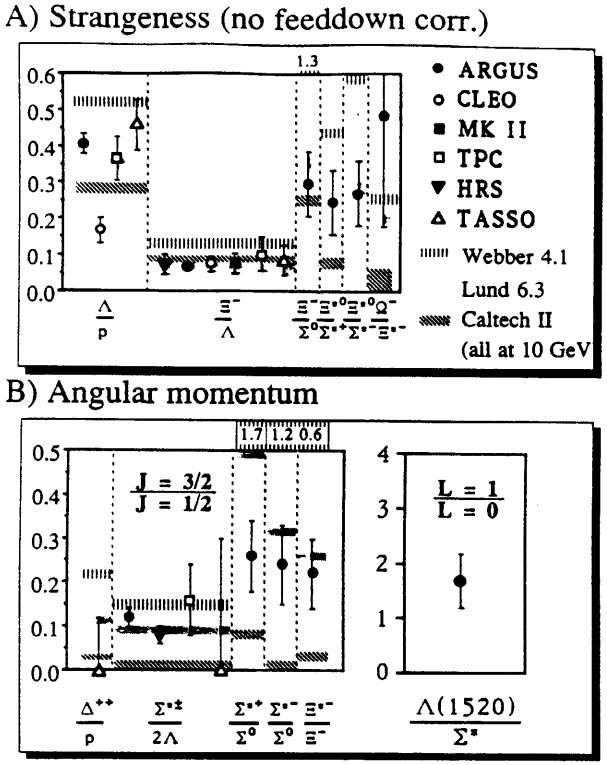

Figure 17: Compilation of baryon production ratios at 10 — 35 GeV, compared with Webber (HERWIG precursor), Lund (JETSET) and CALTECH-II predictions at 10 GeV, for baryons with varying (a) strangeness content, and (b) angular momentum [84].

terms of $z = n/\langle n \rangle$ (multiplicity over average multiplicity), the distribution is independent of CM energy, to a good degree of accuracy — KNO scaling [81]. This is less trivial than it may sound. It has been shown that, at asymptotic energies, the parton shower gives rise to an approximate negative binomial parton multiplicity distribution which KNO scales [82]. At currently explored energies the parton distribution is narrower, and does not KNO scale with energy. However, here fragmentation effects induce an additional broadening of the multiplicity distribution. Only the sum of the two contributions gives approximate KNO scaling over a wide range of energies [83]. In the framework of the parton shower plus string fragmentation model, the crossover between the fragmentation dominated and the shower dominated region is at around 50 GeV.

4.3.2 Particle composition

So far, no LEP results have been presented on the particle composition of events. From PETRA/PEP energies, a reasonably complete experimental picture has emerged [84,16], which thus remains to be tested. Noteworthy is that none of the existing fragmentation models does more than a passable job in describing the baryon composition, Fig. 17. JETSET does least bad, but contains quite a few parameters. CALTECH-II

is about as wasteful with parameters, and still does not fit. The cluster decay of HERWIG is the only economical model, since the particle composition is given by the showering history and simple phase space considerations, but this program does worst.

Given the current state of affairs, there have been some attempts to find alternative descriptions. In the UCLA variation of the Lund model [85], the probability to produce different hadrons is determined by the integral of the Lund symmetric fragmentation function over all z values, i.e. by a monotonically decreasing function of the hadron mass, times Clebsch-Gordan coefficients of the quark content. Quark and diquark masses do not enter the game. This gives a description of comparable quality to the standard Lund one, but with significantly fewer parameters.

Disregarding the problems with the absolute normalizations, the momentum spectra of particles are reasonably well described. However, a closer look reveals problems e.g. in the p/π ratio as a function of particle momentum [86]; this distribution is not quite well described in either existing model.

4.3.3 Intermittency

One of the most discussed topics in recent years has been that of 'intermittency' [87,65,3], a term borrowed from the theory of turbulence. In high energy physics, it is used to denote multiplicity fluctuations which become stronger the smaller the regions of phase space considered. To distinguish trivial and non-trivial fluctuations, one introduced factorial moments [87]. If, e.g., the total rapidity range Y is divided into M bins, each with a width $\delta y = Y/M$, then the i:th factorial moment is defined as

$$F_i(\delta y) = \frac{M^{i-1}}{\langle N \rangle^i} \left\langle \sum_{m=1}^{M} n_m(n_m - 1)\cdots(n_m - i + 1) \right\rangle, \tag{31}$$

where n_m is the multiplicity in bin m, N is the total multiplicity and $\langle \cdots \rangle$ indicates average over all events in the sample. Slightly different averaging procedures are possible, but they all share the same basic properties. The factoral moments are constructed such that they are identically equal to unity for a longitudinal phase space model with purely Poissonian multiplicity fletuations. The signal for 'true intermittency' is that the factorial moments keep on increasing as M is made larger, according to a power law behaviour, $F_i \propto (Y/\delta y)^{f_i} = M^{f_i}$.

However, there are also sources of 'false intermittency', where an approximate power law behaviour may be observed over a range of δy values, but where asymptotically F_i goes to a constant:

- Resonance production.
- Non-flat rapidity distributions, from edge effects, event axis determinations, particle misidentifications, etc.
- Jet production.
- Bose-Einstein effects.

(The list above does not include purely experimental problems, e.g. that a track with a kink may be reconstructed as two separate nearby tracks.) The first two effects typically contribute mainly for $\delta y > 1$, while the last one is believed to give only minor contributions in current studies. The main effect therefore is jet production: if a jet is produced at a given rapidity, its fragmentation will give rise to several hadrons close to this rapidity. Since the typical transverse width of a jet is at around 1 GeV, factorial moments will increase down to scales of $\delta y \approx (1\ \text{GeV})/p_{T_{jet}}$, where $p_{T_{jet}}$ is the tranverse momentum of the jet with respect to the event axis. The amount of 'false intermittency' increases with the CM energy, since the phase space for gluon emission becomes larger.

It is a general misconception that an intermittency signal from jets has to be related to cascading, specifically to parton shower evolution. Even if only three-jet events were

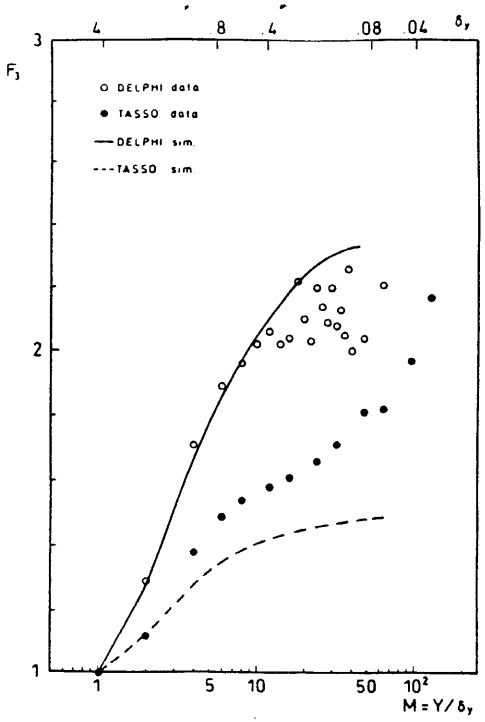

Figure 18: The third factorial moment as a function of the number of bins, TASSO 35 GeV and DELPHI 91 GeV data (circles) compared with JETSET shower + string fragmentation program at the same energies (lines) [91].

produced, i.e. events with no intermittency on the parton level, the fragmentation process would give particles at nearby rapidities, and hence rising factorial moments. In fact, the introduction of a parton shower picture rather leads to a broadening of jet profiles and thus to a reduction of factorial moments compared to the three-jet case [88].

Signals for intermittency were first observed in hadronic collisions. The first indirect evidence in e^+e^- came from an analysis of HRS data [89]. Later the TASSO analysis showed that programs like JETSET and HERWIG, when tuned to describe other data, cannot describe the factorial moments [90]. The disagreement is both in the variation as a function of δy and in the absolute level. In particular, the data points keep on rising for very small bin sizes, where the models tend to flatten out, see Fig. 18.

At LEP energies, so far only DELPHI has presented an intermittency analysis [91]. Contrary to TASSO, good agreement is observed between models and data, both in absolute level and in a tendency for F_i distributions to flatten out at small bin sizes, Fig. 18. If the analysis is extended to a simultaneous binning in both rapidity and azimuth, the factorial moments do not seem to flatten out, but again data and Monte Carlo follow suit.

The discrepancy between TASSO and DELPHI does not seem to be just a matter of having experiments at different energies, since recently CELLO has presented data taken at the same energy as TASSO, which disagrees with TASSO but agrees with model predictions [92]. One cannot exclude the possibility that the TASSO analysis

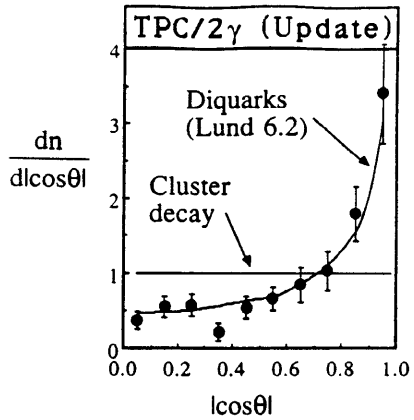

Figure 19: Distribution in $|\cos\theta|$, with θ the angle between the event axis and the $p\bar{p}$ axis in the rest frame of the pair; TPC/2γ data compared with isotropic cluster decay and JETSET baryon production [93,84].

is flawed, so the conservative judgement would be that intermittency in e^+e^- still remains to be convincingly demonstrated.

Finally, a personal comment on this controversial issue. People in the field have developed a terminology of their own, which still is evolving rapidly. A year ago, a factorial moments distribution had to have a power law rise at asymptotically small bin sizes to be called intermittent. By now it has been shown that a distribution, which follows a power law in three dimensions, may have projections on one dimension which flatten out at small bin sizes. Therefore any factorial moments distribution which shows an increase over some significant region of δy values, like the DELPHI ones do, today automatically is called intermittent. However, *if* the LEP data can be perfectly well described by the standard parton shower plus fragmentation pictures, then to use the intermittency language is rather uneconomical and imprecise, however 'photogenique' the term may be. It is the belief of this author that e^+e^- annihilation may not be the right process in which to look for 'true' intermittency, whatever that is, but that the challenge is to be found in the understanding of hadron collision data.

4.3.4 Baryon pair correlations

Flavour correlations have not yet been studied at LEP. At lower energies, nontrival results have been obtained. A particularly useful probe is baryon correlations, since baryons are rare enough that usually only one baryon-antibaryon pair is present in an event, and baryons are also less affected by resonance decays.

One example is the TPC/2γ study of the distribution in the opening angle θ between the event axis and the internal axis of the $p\bar{p}$ pair, the latter axis defined by boosting to the rest frame of the $p\bar{p}$ pair [93,84]. In a cluster fragmentation picture, where clusters are not assumed to have any net baryon number, a flat distribution is expected in $\cos\theta$, slightly modified by events with several baryon-antibaryon pairs. Instead the data show a strong peaking at $\cos\theta = \pm 1$, Fig. 19, as predicted in the Lund model, where the baryon and antibaryon are pulled apart along the string direction.

Further, correlation studies have indicated that when baryons are produced, they do not predominantly appear as nearest neighbours in rank (i.e. sharing a diquark-antidiquark pair), but rather are separated by at least one intermediate meson most of the time.

4.4 Jet Type Separation

4.4.1 Heavy vs. light quark jets

Not all quark jets are expected to be the same. Among the light u, d, and s quarks, differences are expected to reflect the different charge and strangeness content. If quark and antiquark jets are averaged over, and if π/K mesons are not separated, such differences are minor, however.

The situation is more interesting for the heavier c and b quark jets. Here it is well established that the heavy flavour jet deposits a major fraction of its energy into the leading charm or bottom hadron, and that this fraction is larger the heavier the quark is. This is most succinctly expressed by the Bjorken formula [94]

$$\langle z \rangle \approx 1 - \frac{1\ \mathrm{GeV}}{m_Q}, \tag{32}$$

where m_Q is the heavy flavour quark mass and $\langle z \rangle$ is the fraction of total jet energy (or momentum) taken by the heavy flavour hadron. The philosophy underlying this formula is that heavy quarks are not expected to be significantly decelerated during the fragmentation process.

Many explicit fragmentation functions have been based on this principle, the most famous being the Peterson *et al.* one [95],

$$f(z) \propto \left[z \left(1 - \frac{1}{z} - \frac{\epsilon_Q}{1-z} \right)^2 \right]^{-1}, \tag{33}$$

which is based on arguments in old-fashioned perturbation theory for the process $Q \to H(= Q\overline{q}) + q$. Here one expects $\epsilon_Q = (m_0/m_Q)^2$, with m_0 some reference scale related to light hadrons.

The Lund symmetric fragmentation function, eq. (23), is the only publicly propounded function which breaks the Bjorken relation. Instead the asymptotic behaviour here is given by

$$\langle z \rangle \approx 1 - \frac{1+a}{bm_H^2}, \tag{34}$$

with a and b the same parameters as used for ordinary light hadrons, and m_H the mass of the heavy hadron. Compared to the Bjorken approach, differences are not large for charm hadrons, while the Lund picture predicts a harder fragmentation function for B mesons.

The discussion above only covers the nonperturbative fragmentation aspects. In addition, it is necessary to take into account the effects of gluon emission, e.g. in the framework of one of the standard parton shower programs (for a recent analytical evaluation, see [96]). The gluon emission effects increase with increasing CM energy, and lead to a continuous softening of the observable fragmentation function.

At PETRA energies, data were not precise enough to really distinguish between the Bjorken-Peterson and the Lund philosophies, although some slight preference could be given to the former [97]. The ratio of $b\overline{b}$ to $c\overline{c}$ events is considerably more favourable at LEP, and so experiments have been able rapidly to present some first results on the average z value of B hadrons (indirectly, by studying lepton spectra) [98]. These values agree well with extrapolations from lower energies of the Peterson function [3], but are significantly softer than the predictions obtained with the Lund fragmentation function.

This means that some of the assumptions of the Lund approach have to be reexamined, at least for the case of heavy flavours. Other string-based fragmentation functions have been proposed, in particlar by Bowler [99] (derived in the framework

of the Artru-Mennessier model, see section 3.1.2):

$$f(z) \propto \frac{1}{z^{1+bm_Q^2}} \exp(-bm_T^2/z). \tag{35}$$

(It would be possible to motivate the introduction of a $(1-z)^a$ term, to bring the form even closer to the standard Lund one [63].) There is some hope that this could provide a viable string alternative to the Peterson function. Obviously, once the actual shape of the fragmentation function is measured well, rather than just $\langle z \rangle$, it should be possible to differentiate better between the alternatives.

4.4.2 Gluon vs. quark jets

The gluon has a larger colour charge than a quark has. In perturbative QCD this is reflected in a larger probability for a gluon to radiate: referring back to the Altarelli-Parisi splitting kernels of eq. (18), the ratio of gluon to quark bremsstrahlung probability is roughly $N_C/C_F = 9/4$. The difference in colour charge should also be reflected in the nonperturbative treatment, as in the Lund string model, where a gluon is attached to two string pieces but a quark only to one. Altogether, there is therefore strong theoretical support for the idea that a gluon jet ought to have a softer particle distribution than a quark jet of the same energy.

A number of factors act to obscure the theoretical picture: the naive factor of two multiplicity difference between quark and gluon jets is only expected at very large energies; presence of heavy quarks tend to soften the average quark jet, while comparisons with gluons should properly be made for light quarks only; it is difficult to know which is the gluon jet in a three-jet event; etc. It is therefore maybe not surprising that it has turned out to be very difficult to establish such differences.

Gluon jet identification problems can be avoided by comparing symmetric three-jet events at some CM energy with two-jet events at two thirds of this energy. If a fragmentation function per jet is defined in the two cases, tha ratio of these two functions should be unity if quark and gluon jets fragment the same way. Mark II found a ratio below unity at large x (i.e. for particles with large momenta) and above unity at small x [100], consistent with gluon jets being softer than quark ones. A corresponding study by TASSO gave ratios close to unity at all x values [101], in disagreement with the Mark II result. However, it seems this contradiction is mainly an issue of different experimental procedures: also the ratios predicted by various programs differ between Mark II and TASSO, in the same way as the data itself. Thus the HERWIG (Webber) program agrees well with both data sets, while the JETSET matrix element option gives too large a ratio at large x. This indicates that it is necessary to have gluon jets softer both by the shower evolution stage and by the fragmentation one. Softer fragmentation alone, as in the JETSET matrix element option, is not enough. Simple independent fragmentation, with $g = q$, fares even worse.

The alternative procedure is to look at asymmetric three-jet events, and assume the jet with lowest energy to be the gluon one, cf. the discussion of string effects below. This technique has been much used in the past, with varying success. The most recent and detailed study is by AMY [102], where a number of characteristics of the three jets are compared, such as the fraction of the total jet energy found in the core of the jet, the rapidity of the leading particle, and the integral of the Energy-Energy Correlation for small relative angles between particles. All these measures show that the lowest energy jet is softer than the other two are, above and beyond what is expected simply from the differences in jet energies. Unfortunately, the study is based on limited statistics.

With the larger jet energies and huge statistics available at LEP, this is obviously one area where one would expect more detailed studies in the future, so that the

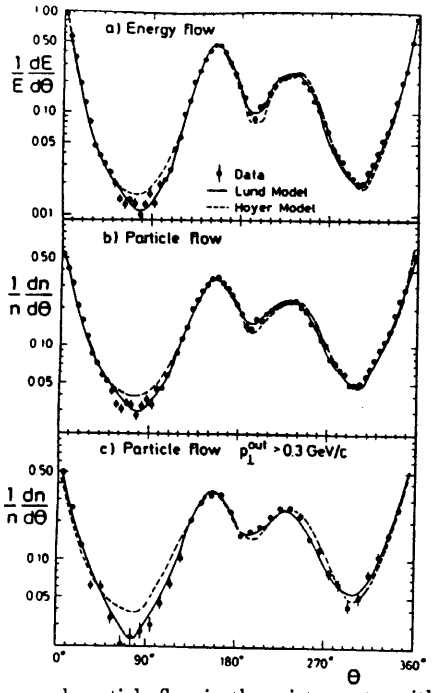

Figure 20: Energy and particle flow in three-jet events, with the leftmost valley likely to correspond to the q–$\bar{q}$ angular region. JADE data compared with the Lund string model and the Hoyer independent fragmentation one [104].

differences between quark and gluon jets could be pinned down unambiguously.

4.5 String and Coherence Phenomena

In a three-jet event, the Lund model is based on having a string stretched from the quark via the gluon to the antiquark. Fig. 10. The string piece between the quark and the gluon has a transverse motion out along a direction intermediate to the quark and gluon directions. The particles which are produced when the string piece breaks therefore receive a Lorentz boost, such that slow particles systematically are shifted slightly away from the origin. A corresponding boost in a direction intermediate to the gluon and antiquark directions is required for the string piece spanned by these two partons. Since there is not a string piece spanned directly between the quark and antiquark, no particles are produced in between these two partons, except by 'leakage' from the other two regions, by transverse momentum fluctuations and particle decays. In the Lund string picture, there is therefore a direct prediction that the region between the quark and antiquark directions should be significantly less populated than the two other regions between jets [103]. This contrasts with the behaviour in the independent fragmentation framework, where fragmentation takes place symmetrically around each of the three jet directions, and therefore none of the three regions between jets occupies a special position.

Comparisons with data have tended to favour the Lund scenario, and disfavour the independent fragmentation one [104]. One example of this kind of studies is shown in Fig. 20. The effects that are experimentally observed are actually much smaller

than the ones predicted on the Monte Carlo level — it is difficult to know which jet is the gluon one, and therefore the true effect is reduced by the influence of events where the gluon is misidientified. So far, essentially all studies have been based on the assumption that the jet with lowest energy is the gluon one, which typically is true only 60% of the time. With the much higher statistics promised by LEP one could consider more reliable methods, such as to tag the quark and antiquark of an event by the presence of prompt leptons from semileptonic charm and bottom decays. Even so, the experimental evidence is fairly convincing, and few models manage to describe the data.

The Leningrad group has shown that the 'string effect' appears as a natural consequence of coherence phenomena in the parton shower evolution [39]. In lowest order, this may be viewed as follows. Start out with a quark, an antiquark and a gluon, all three with approximately the same energy, and let the three partons act as antennae that emit soft gluons in a semiclassical pattern. Due to interference effects between the colour charges of the three partons, there is then a surplus of radiation in the q–g and g–$\bar{q}$ regions, and a depletion in the q–$\bar{q}$ one. If a term proportional to $1/N_C$ (i.e. a colour suppressed term) is dropped, the two remaining terms may be interpreted as simple qg and $\bar{q}g$ dipole radiation, boosted from the the qg and $\bar{q}g$ rest frames into the overall $q\bar{q}g$ CM frame.

The scenario above literally repeats the explanation given in the string model, with the important difference that, where the string picture is based on purely nonperturbative deliberations, the colour antennae picture is purely perturbative. Despite the sharing of a common ideological basis, namely the importance of the colour flow in events, the two explanations are not describing quite the same physics. The perturbative and nonperturbative scenarios can be distinguished by more detailed tests, tests which can be carried out by comparing data at LEP with those from lower energies. Some examples can be found in [105], but here we will present another one [106].

Consider, for simplicity, a symmetric three-jet event. Denote by E_{qg} $(= E_{\bar{q}g})$ the energy flow in the middle of the angular region between the q and g jet directions (e.g. integrated over the central $0.4 \cdot 120° = 48°$ of this region), and by $E_{q\bar{q}}$ the corresponding energy flow between the q and $\bar{q}$ jet directions. In the string picture, E_{qg} and $E_{q\bar{q}}$ are essentially independent of the CM energy: as the energy is increased, more particles are produced along the three jet directions (at large momenta), but the center of the string pieces between the jets remain the same. In the perturbative framework, on the other hand, it is the *fraction* of energy radiated into gluons between the jets that stays the same, modulo the running of α_S and issues related to the cutoff of the shower evolution at low virtualities. One therefore expects $E_{qg}, E_{q\bar{q}} \propto \alpha_S E_{CM}$. In forming the ratio $E_{qg}/E_{q\bar{q}}$, as has traditionally been done, the energy dependence is factored out, so that both approaches predict a constant ratio as function of CM energy.

The energy difference, $\Delta E = E_{qg} - E_{q\bar{q}}$, however, preserves the contrast between the two approaches. This is illustrated in Fig 21. Furthermore, it allows for a world in which not all is 'black and white', but where both perturbative and nonperturbative contributions coexist. In fact, in the full JETSET simulation, which includes both parton shower evolution and string fragmentation, it turns out that the two contributions add up more or less incoherently. It would therefore be motivated to fit data at different energies to a form

$$\Delta E(E_{CM}) = E_{qg}(E_{CM}) - E_{q\bar{q}}(E_{CM}) = c_1 + c_2 \alpha_S E_{CM}. \tag{36}$$

The presence of both these terms in the data would thus demonstrate the complementary nature of the perturbative and the nonperturbative contributions. Obviously, perturbative effects are guaranteed to win out eventually, but LEP is still at around the crossover point (if the JETSET simulations are to be believed), and so is ideally placed to address this kind of issues. Needless to say, the experimental problems are considerable, in particular since gluon jet misidentifications significantly reduce

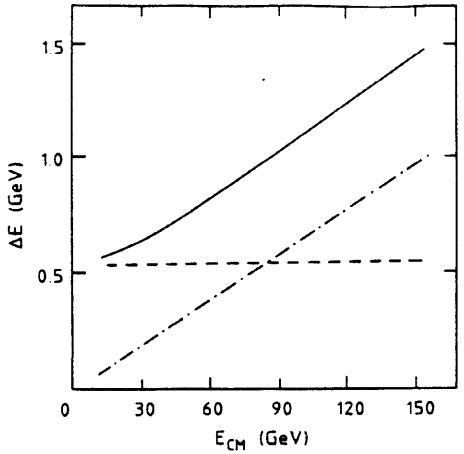

Figure 21: The difference ΔE of energy flows in the q–g and q–$\bar{q}$ angular ranges of symmetric three-jet events. In this figure only u and d quarks are included, and α_S is chosen fix. = 0.20. No jet misidentification or other experimental problems are included. The dashed line shows string fragmentation of three-jets only, the dashed-dotted line the energy flow on the parton level in a parton shower approach, and the full curve the hadronic energy flow when parton shower evolution is followed by string fragmentation. All curves have been obtained with JETSET.

observable effects, and since it is necessary to compare data obtained with different detectors operating at different energies. If nothing else, the discussion above provides a 'gedanken experiment', to help understand the distinction between perturbative and nonperturbative effects better.

The coherence phenomenon gives a reduction of the amount of soft gluon emission, compared to non-coherent scenarios [32,30,26]. If the distribution of hadrons follows that of the partons, like in the framework of local parton-hadron duality, it is possible to give precise analytical formulae for the shape of the momentum distribution of particles, at least in the region around the maximum of the $\ln(1/x_p)$ distribution, where $x_p = 2p/E_{CM}$ is the momentum fraction of a particle. This distribution has been studied by OPAL [107], and good agreement is found with analytical predictions, as well as with Monte Carlo results. Further, the evolution of the peak position of the $\ln(1/x_p)$ distribution from TASSO [77] to OPAL energies is well described. In a model based on incoherent shower evolution and independent fragmentation the energy dependence can not be reproduced. Since the purely nonperturbative string fragmentation model has the property of depleting the low-momentum region in multijet events just by the string effect, a model based on non-coherent shower evolution plus string fragmentation can give a reasonable description of data at any fix energy, but it fails to get the energy dependence quite right.

It is also interesting to consider the rapidity distribution of particles. This distribution has a characteristic dip in the region around rapidity zero, see Fig. 16. While coherence phenomena contribute to this dip, the main contribution comes from the choice of event axis (usually based on thrust, which has known pathologies in this respect), from the non-identification of kaons and protons (these therefore are assumed to have the pion mass), and from heavy flavour decays. It is difficult to disentangle the different contributions experimentally. However, if particles are correctly identified, and if the rapidity distribution is plotted separately for different sphericity bins,

TPC/2γ has shown [108] that the dip is absent at small or large sphericities, i.e. only present for events that are somewhere in between the simple two-jet and the clearcut multijet ones. In other words, the dip is related to the emission of soft and/or collinear partons. This behaviour is predicted in models based on coherent showers plus string fragmentation, but can not be reproduced by independent fragmentation models, and only poorly by matrix elements plus string fragmentation.

5 Summary and Outlook

The perturbative aspects of QCD are fairly well under control. The running of α_S and the structure of the fundamental couplings of QCD (with the exception of the four-gluon one) have already been successfully tested at LEP (with some backing from PETRA/PEP/TRISTAN data). In the light of the issue of optimized Q^2 scales, one may have different opinions about how well α_S is really determined, but this does not affect how well physical quantities can be predicted.

The matrix element approach has made a remarkable comeback. For a long time it was considered dead as a viable alternative for the description of event shapes at LEP energies. In particular, the lack of four-jet events was a serious shortcoming. The wholehearted adoption of optimized perturbation theory has at least solved that problem. If fragmentation parameters are retuned, i.e. if soft gluon effects are bundled together with the nonperturbative fragmentation description, it is even possible to get quite acceptable descriptions of the generic event properties studied so far.

We should not be swept off our feet by these successes, however. The estimate of higher order effects by the use of optimized Q^2 scales is no substitute for a full-length actual calculation of, in particular, the loop corrections to the four-jet rate. Furthermore, the need for quite a significant retuning of fragmentation parameters when going from PETRA/PEP to LEP energies shows that the effects of soft gluons, which are not included in the matrix element treatment, are large.

The alternative perturbative description is the parton shower one. Originally, this approach had no particular claim to accurate predictions, but with time the level of ambition has increased. We may reasonably expect further progress in the future, although the pace may be slower than in the past. One particular advantage of the parton shower approach is that we expect all model parameters to be independent of the CM energy. This indeed seems to be the case experimentally, which gives us confidence in predicting event shapes at energies beyond what has been observed so far.

On the fragmentation side, there used to be three competing models. Of these, independent fragmentation no longer is a serious alternative, but occasionally still is used as a contrast to the other two. Cluster fragmentation in principle is the model with least free parameters, but the minimal forms of the cluster model have not been very successful in accounting for the data. String fragmentation, on the other hand, contains many parameters, but also gives quite a good description of most data. In fact, at LEP, only one spectacular failure has been registered so far: the bottom fragmentation function is distinctly softer than predicted. Much of the evolution in the cluster models has been attempts to make them more stringlike. It is not unreasonable that 'the truth' lies somewhere in between the two extremes but, judging by our current experience, rather closer to the string approach.

If parton shower models still show a healthy learning curve upwards, the same cannot really be said about fragmentation models. Very little visible progress has been made in the last five years. Specifically, we see no 'fourth alternative' on the horizon, which could take up competition with our currently known three approaches. Further, the task of connecting up these models with a more solid understanding of nonperturbative QCD still lies ahead of us.

The study of QCD at LEP, perturbative and nonperturbative, is off to a good start. The 'shopping list', which is now being worked on, includes items like:

- Perturbative QCD.
  - The running of α_S and other scaling violations.
  - Studies of the fundamental vertices of QCD (specifically the triple-gluon vertex).
  - Improved understanding of the region of validity of optimized perturbation theory.
  - Exponentiation of matrix elements (i.e. introduction of Sudakov form factors).
- Coherence effects (mainly perturbative, but with some nonperturbative ingredients).
  - Momentum and rapidity distributions.
  - Particle and energy flow in three-jet events (including flavour dependence).
  - Other particle and energy flow correlations, e.g. as proposed in [109].
- Differences between jet types.
  - Gluon versus quark jets.
  - Heavy flavour fragmentation functions.
  - Flavour tagging (also for studies of electroweak couplings).
- Multiplicities and correlations.
  - Increase of average multiplicity with energy.
  - Shape of multiplicity distribution, in the event as a whole, and in rapidity windows.
  - Probability of having a very low multiplicity in a jet.
  - Intermittency, in one and several dimensions.
  - Bose-Einstein effects.
- Flavour properties.
  - Particle composition and its consistency with results at lower energies.
  - Rate of rare baryon production.
  - Baryon-antibaryon correlations.
  - Importance of tensor mesons and other excited states.
- Prompt photon production [110].
  - As probe of the primary flavour composition.
  - As probe of parton showering.

It would be unrealistic to assume that a revolutionary change of our understanding of strong interactions will come out of LEP studies. QCD is already too well entrenched for that. This should not unduly discourage us. Many aspects of QCD are still poorly understood, in particular in the semisoft and soft regions. Here LEP will be an excellent laboratory for increasing our understanding over the years to come.

Acknowledgements

Thanks to the organizers of the Cargèse meeting for having arranged two wonderful weeks of physics and sun. Thanks to the organizers of the Santander meeting for a stimulating conference and interesting visits. Also thanks to S. Bethke and V. Khoze for helpful comments on parts of the manuscript.

References

[1] see e.g. G. Altarelli, Phys. Rep. **81** (1982) 1
[2] R. Kleiss *et al.*, *in* eds. G. Altarelli, R. Kleiss, C. Verzegnassi, CERN 89-08, volume 3, p. 1,
as well as several reports in volume 1
[3] T. Sjöstrand *et al.*, *ibid.*, volume 3, p. 143
[4] Z. Kunszt *et al.*, *ibid.*, volume 1, p. 373
[5] J. Ellis, M.K. Gaillard, G.G. Ross, Nucl. Phys. **B111** (1976) 253
[6] T. Sjöstrand, Z. Physik **C26** (1984) 93
[7] A. Ali, J.G. Körner, Z. Kunszt, E. Pietarinen, G. Kramer, G. Schierholz, J. Willrodt, Nucl. Phys. **B167** (1980) 454
[8] K.J.F. Gaemers, J.A.M. Vermaseren, Z. Physik **C7** (1980) 81
[9] R.K. Ellis, D.A. Ross, A.E. Terrano, Nucl. Phys. **B178** (1981) 421
[10] D. Danckaert, P. De Causmaecker, R. Gastmans, W. Troost, T.T. Wu, Phys. Lett. **114B** (1982) 203
[11] B.A. Kniehl, J.H. Kühn, Phys. Lett. **B224** (1989) 229
[12] J.A.M. Vermaseren, K.J.F. Gaemers, S.J. Oldham, Nucl. Phys. **B187** (1981) 301
[13] K. Fabricius, G. Kramer, G. Schierholz, I. Schmitt, Z. Physik **C11** (1982) 315
[14] Z. Kunszt, Phys. Lett. **99B** (1981) 429, **107B** (1981) 123;
T.D. Gottschalk, Phys. Lett. **109B** (1982) 331;
R.-y. Zhu, MIT Ph.D. thesis (1983);
A. Ali, F. Barreiro, Nucl. Phys. **B236** (1984) 269;
F. Gutbrod, G. Kramer, G. Schierholz, Z. Physik **C21** (1984) 235;
T.D. Gottschalk, M.P. Shatz, Phys. Lett. **150B** (1985) 451, CALT-68-1172 (1984);
G. Kramer, B. Lampe, Fortschr. Phys. **37** (1989) 161;
F. Gutbrod, G. Kramer, G. Rudolph, G. Schierholz, Z. Physik **C35** (1987) 543
[15] G. Kramer, N. Magnussen, DESY 90-080
[16] Particle Data Group, J.J. Hernández *et al.*, Phys. Lett. **B239** (1990) 1
[17] M. Dine, J. Sapirstein, Phys. Rev. Lett. **43** (1979) 668;
K.G. Chetyrkin *et al.*, Phys. Lett. **85B** (1979) 277;
W. Celmaster, R.J. Gonsalves, Phys. Rev. Lett. **44** (1980) 560
[18] S.G. Gorishny, A.L. Kataev, S.A. Larin, Phys. Lett. **B212** (1988) 238
[19] JADE Collaboration, W. Bartel *et al.*, Z. Physik **C33** (1986) 23
[20] JADE Collaboration, S. Bethke *et al.*, Phys. Lett. **B213** (1988) 235;
TASSO Collaboration, W. Braunschweig *et al.*, Phys. Lett. **B214** (1988) 286;
Mark II Collaboration, S. Bethke *et al.*, Z. Physik **C43** (1989) 325;
AMY Collaboration, I.H. Park *et al.*, Phys. Rev. Lett. **62** (1989) 1713;
VENUS Collaboration, K. Abe *et al.*, Phys. Lett. **B240** (1990) 232
[21] OPAL Collaboration, M.Z. Akrawy *et al.*, Phys. Lett. **B235** (1990) 389, CERN-PPE/90-143;
DELPHI Collaboration, P. Abreu *et al.*, Phys. Lett. **B247** (1990) 167;
L3 Collaboration, B. Adeva *et al.*, L3 Preprint #011 (1990)
[22] P.M. Stevenson, Phys. Rev. **D23** (1981) 2916
[23] G. Grunberg, Phys. Lett. **95B** (1980) 70
[24] S.J. Brodsky, G.P. Lepage, P.B.Mackenzie, Phys. Rev. **D28** (1983) 228
[25] M. Jacob, rapporteur talk at the 25th International Conference on High Energy Physics, Singapore, 2–8 August, 1990
[26] Yu.L. Dokshitzer, V.A. Khoze, S.I. Troyan, Sov. J. Nucl. Phys. (Yad. Fiz.) **47** (1988) 1384, *in* Perturbative QCD, ed. A.H. Mueller (World Scientific, Singa-

pore, 1989), p. 241
[27] K. Hagiwara, D. Zeppenfeld, Nucl. Phys. **B313** (1989) 560;
N.K. Falck, D. Graudenz, G. Kramer, Phys. Lett. **B220** (1989) 299, Nucl. Phys. **B328** (1989) 317
[28] F.A. Berends, W.T. Giele, H. Kuijf, Nucl. Phys. **B321** (1989) 39
[29] C. J. Maxwell, Phys. Lett. **B225** (1989) 425
[30] A.H. Mueller, Nucl. Phys. **B213** (1983) 85, **B241** (1984) 141;
Yu.L. Dokshitzer, S.I. Troyan, Leningrad preprint LNPI-922 (1984);
A. Bassetto, M. Ciafaloni, G. Marchesini, Phys. Rep. **100** (1983) 201;
B.R. Webber, Ann. Rev. Nucl. Part. Sci. **36** (1986) 253
[31] G. Altarelli, G. Parisi, Nucl. Phys. **B126** (1977) 298
[32] A.H. Mueller, Phys. Lett. **B104** (1981) 161;
B.I. Ermolaev, V.S. Fadin, JETP Lett. **33** (1981) 269
[33] A.E. Chudakov, Izv. Akad. Nauk SSSR, Ser. Fiz. **19** (1955) 650
[34] G. Marchesini, B.R. Webber, Nucl. Phys. **B238** (1984) 1;
B.R. Webber, Nucl. Phys. **B238** (1984) 492;
G. Marchesini, B.R. Webber, Nucl. Phys. **B310** (1988) 461
[35] M. Bengtsson, T. Sjöstrand, Phys. Lett. **B185** (1987) 435, Nucl. Phys. **B289** (1987) 810
[36] J.C. Collins, Nucl. Phys. **B304** (1988) 794;
I.G. Knowles, Nucl. Phys. **B310** (1988) 571
[37] K. Kato, T. Munehisa, Phys. Rev. **D39** (1989) 156, CERN-TH.5719/90
[38] G. Gustafson, Phys. Lett. **B175** (1986) 453;
G. Gustafson, U. Pettersson, Nucl. Phys. **B306** (1988) 746;
L. Lönnblad, Lund preprint LU TP 89-10 (1989)
[39] Ya.I. Azimov, Yu.L. Dokshitzer, V.A. Khoze, S.I. Troyan, Phys. Lett. **B165** (1985) 147, Yad. Fiz. **43** (1986) 149
[40] J. Ellis, I. Karliner, Nucl. Phys. **B148** (1979) 141
[41] TASSO Collaboration, R. Brandelik *et al.*, Phys. Lett. **97B** (1980) 453
[42] S. Bethke, LBL-28112 (1989)
[43] T.F. Walsh, P.M. Zerwas, Phys. Lett. **93B** (1980) 53
[44] W.M. Geist, D. Drijard, A. Putzer, R. Sosnowski, D. Wegener, CERN/EP 89-159 (to appear in Phys. Rep.), and references therein
[45] J.G. Körner, G. Schierholz, J. Willrodt, Nucl. Phys. **B185** (1981) 365;
O. Nachtmann, A. Reiter, Z. Phys. **C16** (1982) 45;
M. Bengtsson, P.M. Zerwas, Phys. Lett. **B208** (1988) 306;
M. Bengtsson, Z. Phys. **C42** (1989) 75;
S. Bethke, A. Ricker, P.M. Zerwas, Aachen preprint PITHA 90/14 (1990)
[46] OPAL Collaboration, M.Z. Akrawy *et al.*, CERN-PPE/90-97 (1990)
[47] L3 Collaboration, B. Adeva *et al.*, Phys. Lett. **B248** (1990) 227
[48] DELPHI Collaboration, contribution to the 25th International Conference on High Energy Physics, Singapore, 2–8 August, 1990;
H. Müller, parallel session talk at this conference
[49] AMY Collaboration, I. H. Park *et al.*, Phys. Rev. Lett. **62** (1989) 1713;
VENUS Collaboration, K. Abe *et al.*, KEK Preprint 90-62 (1990)
[50] T. Sjöstrand, Int. J. Mod. Phys. **A3** (1988) 751
[51] X. Artru, G. Mennessier, Nucl. Phys. **B70** (1974) 93
[52] B. Andersson, G. Gustafson, G. Ingelman, T. Sjöstrand, Phys. Rep. **97** (1983) 31
[53] X. Artru, Phys. Rep. **97** (1983) 147
[54] G. Gustafson, Z. Physik **C15** (1982) 155

[55] G. Gustafson, U. Pettersson, P. Zerwas, Phys. Lett. **B209** (1988) 90
[56] A. Krzywicki, B. Petersson, Phys. Rev. **D6** (1972) 924;
J. Finkelstein, R.D. Peccei, Phys. Rev. **D6** (1972) 2606;
F. Niedermayer, Nucl. Phys. **B79** (1974) 355;
A. Casher, J. Kogut, L. Susskind, Phys. Rev. **D10** (1974) 732
[57] R.D. Field, R.P. Feynman, Nucl. Phys. **B136** (1978) 1
[58] P. Hoyer, P. Osland, H.G. Sander, T.F. Walsh, P.M. Zerwas, Nucl. Phys. **B161** (1979) 349
[59] A. Ali, J.G. Körner, G. Kramer, J. Willrodt, Nucl. Phys. **B168** (1980) 409;
A. Ali, E. Pietarinen, G. Kramer, J. Willrodt, Phys. Lett. **B93** (1980) 155
[60] I. Montvay, Phys. Lett. **84B** (1979) 331
[61] P. Biddulph, G. Thompson, Computer Physics Commun. **54** (1989) 13;
G. Ballocchi, R. Odorico, CERN-EP/89-162
[62] G.C. Fox, S. Wolfram, Nucl. Phys. **B168** (1980) 285;
R.D. Field, S. Wolfram, Nucl. Phys. **B213** (1983) 65
[63] T.D. Gottschalk, D.A. Morris, Nucl. Phys. **B288** (1987) 729;
D.A.Morris, Caltech Ph.D. thesis, CALT-68-1440 (1987)
[64] D. Amati, G. Veneziano, Phys. Lett. **83B** (1979) 87;
G. Marchesini, L. Trentadue, G. Veneziano, Nucl. Phys. **B181** (1981) 335
[65] W. Kittel, R. Peschanski, Nucl. Phys. **B** (Proc. Suppl.) **16** (1990) 445;
A. Bialas, CERN-TH.5791/90, and references therein
[66] J. Ellis, H. Kowalski, Phys. Lett. **B214** (1988) 161;
J. Ellis, M. Karliner, H. Kowalski, Phys. Lett. **B235** (1990) 341
[67] L. Angelini, L. Nitti, M. Pellicoro, G. Preparata, G. Valenti, Computer Physics Commun. **34** (1985) 371;
W. Ochs, Z. Physik **C23** (1984) 131, **C34** (1987) 397
[68] P. Mättig, Phys. Rep. **177** (1989) 141;
High Energy Electron Positron Physics, eds. A. Ali, P. Söding (World Scientific, Singapore, 1988)
[69] C. Basham, L. Brown, S. Ellis, S. Love, Phys. Rev. Lett. **41** (1978) 1585
[70] S. Brandt, Ch. Peyrou, R. Sosnowski, A. Wroblewski, Phys. Lett. **12** (1964) 57;
E. Fahri, Phys. Rev. Lett. **39** (1977) 1587
[71] J.D. Bjorken, S.J. Brodsky, Phys. Rev. **D1** (1970) 1416
[72] S. Brandt, H.D. Dahmen, Z. Physik **C1** (1979) 61
[73] G. Parisi, Phys. Lett. **74B** (1978) 65;
J.F. Donoghue, F.E. Low, S.Y. Pi, Phys. Rev. **D20** (1979) 2759
[74] T. Sjöstrand, Computer Physics Commun. **28** (1983) 229
[75] ALEPH Collaboration, D. Decamp *et al.*, Phys. Lett. **B234** (1990) 209;
DELPHI Collaboration, P. Aarnio *et al.*, Phys. Lett. **B240** (1990) 271;
OPAL Collaboration, M.Z. Akrawy *et al.*, Z. Physik **C47** (1990) 505
[76] Mark II Collaboration, A. Petersen *et al.*, Phys. Rev. **D37** (1988) 1
[77] TASSO Collaboration, W. Braunschweig *et al.*, Z. Physik **C41** (1988) 359, **C47** (1990) 187
[78] AMY Collaboration, Y.K. Li *et al.*, Phys. Rev. **D41** (1990) 2675
[79] W. de Boer, H. Fürstenau, J.H. Köhne, Karlsruhe preprint IEKP-KA/90-4 (1990)
[80] DELPHI Collaboration, P. Abreu *et al.*, CERN-PPE/90-117
[81] Z. Koba, H.B. Nielsen, P. Olesen, Nucl. Phys. **B40** (1972) 317
[82] E.D. Malaza, B.R.Webber, Nucl. Phys. **B267** (1986) 702;
E.D. Malaza, Z. Physik **C31** (1986) 143
[83] B. Andersson, P. Dahlqvist, G. Gustafson, Z. Physik **C44** (1989) 455

[84] W. Hofmann, Ann. Rev. Nucl. Part. Sci. **38** (1988) 279
[85] C.D. Buchanan, S.-B. Chun, Phys. Rev. Lett. **59** (1987) 1997, *in* Proceedings of the KEK Topical Conference on e^+e^- Collision Physics, eds. Y. Shimizu, F. Takasaki (KEK, Tsukuba, 1990), p. 384
[86] TPC/2γ Collaboration, H. Aihara *et al.*, Phys. Rev. Lett. **61** (1988) 1263; G.D. Cowan, Ph.D. thesis, LBL-24715 (1988)
[87] A. Bialas, R. Peschanski, Nucl. Phys. **B273** (1986) 703, **B308** (1988) 857
[88] T. Sjöstrand, *in* Multiparticle Production, eds. R. Hwa, G. Pancheri, Y. Srivastava (World Scientific, Singapore, 1989), p. 327
[89] B. Buschbeck, P. Lipa, R. Peschanski, Phys. Lett. **B215** (1988) 788
[90] TASSO Collaboration, W. Braunschweig *et al.*, Phys. Lett. **B231** (1989) 548
[91] DELPHI Collaboration, P. Abreu *et al.*, Phys. Lett. **B247** (1990) 137; A. De Angelis, CERN-PPE/90-129
[92] CELLO Collaboration, H.J. Behrend *et al.*, DESY 90-114
[93] TPC/2γ collaboration, H. Aihara *et al.*, Phys. Rev. Lett. **55** (1985) 1047
[94] J.D. Bjorken, Phys. Rev. **D17** (1978) 171; M. Suzuki, Phys. Lett. **71B** (1977) 139; V.A. Khoze, Ya.I. Azimov, L.L. Frankfurt, *in* Proceedings of the Conference on High Energy Physics, Tbilisi 1976
[95] C. Peterson, D. Schlatter, I. Schmitt, P. Zerwas, Phys. Rev. **D27** (1983) 105
[96] B. Mele, P. Nason, Phys. Lett. **B245** (1990) 635
[97] S. Bethke, Z. Physik **C29** (1985) 175, and references therein; J. Chrin, Z. Physik **C36** (1987) 163, and references therein; M. Zimmer, Heidelberg Ph.D. thesis (1989)
[98] L3 Collaboration, B. Adeva *et al.*, Phys. Lett. **B241** (1990) 416; ALEPH Collaboration, D. Decamp *et al.*, Phys. Lett. **B244** (1990) 551
[99] M.G. Bowler, Z. Physik **C11** (1981) 169
[100] Mark II Collaboration, A. Petersen *et al.*, Phys. Rev. Lett. **55** (1985) 1954
[101] TASSO Collaboration, W. Braunschweig *et al.*, Z. Physik **C45** (1989) 1
[102] AMY Collaboration, Y.-K. Kim *et al.*, Phys. Rev. Lett. **63** (1989) 1772; Y.-K. Kim, University of Rochester Ph.D. thesis (1990)
[103] B. Andersson, G. Gustafson, T. Sjöstrand, Phys. Lett. **94B** (1980) 211
[104] A. Petersen (JADE Collaboration), *in* Elementary Constituents and Hadronic Structure, ed. J. Tran Thanh Van (Editions Frontières, Dreux, 1980), p. 505; JADE Collaboration, W. Bartel *et al.*, Phys. Lett. **B101** (1981) 129, **B134** (1984) 275, Z. Physik **C21** (1983) 37; TPC/2γ Collaboration, H. Aihara *et al.*, Z. Physik **C28** (1985) 31; TASSO Collaboration, M. Althoff *et al.*, Z. Physik **C29** (1985) 29
[105] V. Khoze, L. Lönnblad, Phys. Lett. **B241** (1990) 123
[106] T. Sjöstrand, presented at Leningrad QCD workshop, October 1989 (unpublished)
[107] OPAL Collaboration, M.Z. Akrawy *et al.*, Phys. Lett. **B247** (1990) 617
[108] TPC/2γ Collaboration, H. Aihara *et al.*, Z. Physik **C44** (1989) 357
[109] Yu.L. Dokshitzer, V.A. Khoze, G. Marchesini, B.R. Webber, CERN-TH.5694/90
[110] OPAL Collaboration, M.Z. Akrawy *et al.*, Phys. Lett. **B246** (1990) 285

Imprimé au CERN. Prix : 0.85 Fr.